

DANPY (Dimethylaminonaphthylpyridinium): An Economical and Biocompatible Fluorophore

Lewis E. Johnson,^{*,1} Jason S. Kingsbury,^{*,3,‡} Delwin L. Elder,^{1,‡} Rose Ann Cattolico,^{*,2} Luke N. Latimer,¹ William Hardin,² Evelien De Meulenaere,⁴ Chloe Deodato,² Griet Depotter,⁴ Sowmya Madabushi,² Nicholas W. Bigelow,¹ Brittany A. Smolarski,³ Trevor K. Hougen,³ Werner Kaminsky,¹ Koen Clays,⁴ Bruce H. Robinson¹

¹Department of Chemistry, University of Washington, Box 351700, Seattle, WA 98195, U.S.A.

²Department of Biology, University of Washington, Box 351800, Seattle, WA 98195, U.S.A.

³Department of Chemistry, Ahmanson Science Center, California Lutheran University, 60 West Olsen Rd., Thousand Oaks, CA 91360, U.S.A.

⁴Department of Chemistry, Katholieke Universiteit Leuven, Leuven, Belgium B-3001

*Corresponding authors: lewisj@uw.edu (L.E.J., Design and Characterization),

jkingsbu@callutheran.edu (J.S.K., Synthesis), racat@uw.edu (R.A.C., Biology)

‡These authors contributed equally to this work.

† Electronic Supplementary Information available: Detailed synthetic and experimental protocols, ¹H and ¹³C NMR spectra, potential energy surface analysis, detailed crystallographic information, detailed methodology for DNA binding analysis, third-party toxicology data (Ames test, MEM elution cytotoxicity, rabbit irritation test, and mouse systemic toxicity test), nonlinear fitting code, and coordinates for computed structures.

Supporting Information

Table of Contents:

Author contributions – **S2**

Synthesis – **S2**

NMR spectra – **S8**

Infrared and Raman spectra – **S14**

Identity and variation of counterion – **S14**

Crystallography – **S15**

Computational methods – **S18**

Dihedral and molecular orbital analysis - **S18**

Absorbance and fluorescence methodology – **S20**

Two-photon cross section methodology and spectra – **S22**

Photochemical stability – **S24**

DNA binding model/fitting – **S25**

Ethidium Bromide binding curves – **S28**

RNA binding – **S29**

Gel electrophoresis and DNA staining – **S29**

Cell maintenance – **S30**

Microscopic analyses – **S31**

Time-evolution of SHG signal – **S33**

MCFit Nonlinear Fitting Code – **S34**

Coordinates for electronic structure calculations – **S44**

References for supporting information – **S50**

Author Contributions:

Initial project conception – **BHR**

Project design and coordination – **LEJ**

Molecular design and discovery-scale synthesis – **LEJ, LNL**

Synthetic optimization and large-scale synthesis – **JSK, DLE, LEJ, BMS, TLH**

Electronic structure calculations – **LEJ**

Chemical and linear photophysical characterization – **LEJ, DLE, BHR, JSK**

In vitro binding characterization – **LEJ, LNL, BHR, NWB**

Crystallography – **WK**

Hyper-Rayleigh scattering – **GD, KC**

TPA cross-section measurements - **LEJ**

Linear fluorescence microscopy – **WH, RAC**

Flow cytometry – **CD, RAC**

Gel electrophoresis – **SM, RAC**

Nonlinear microscopy – **EDM, KC**

Software development – **LEJ, NWB**

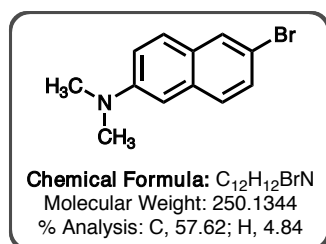
Manuscript writing – **LEJ, JSK, RAC** with contributions by all other authors

Project supervision – **BHR, LEJ, RAC, KC, JSK**

Synthesis:

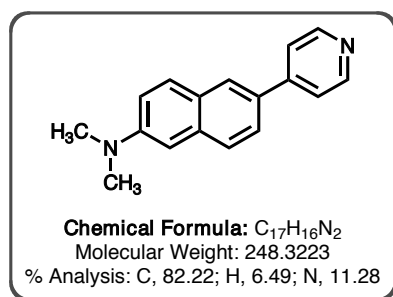
General. All reactions were carried out in oven- and flame-dried glassware under inert atmosphere in dry degassed solvents using Schlenk and vacuum-line techniques. Column chromatography was performed with high purity Davisil™ (grade 635) silica gel (Aldrich). Thin-layer chromatography (TLC) was performed with 0.25 mm thick silica gel 60 F₂₅₄ plates (EMD Chemicals). TLC spot visualization was accomplished by exposure to long- and short-wave ultraviolet light. Infrared spectra were recorded on a Fourier Transform IR spectrophotometer; peaks are reported in wavenumbers (cm⁻¹) as strong (s), medium (m), weak (w), or broad (br). ¹H NMR spectra were recorded on a 500 MHz instrument as part of a user-group consortium established by California State University, Channel Islands (Camarillo, CA). ¹H chemical shifts are listed in ppm from tetramethylsilane with the solvent resonance as the internal standard (CDCl₃ δ 7.26; (CD₃)₂CO δ 2.05; (CD₃)₂SO δ 2.50) in the following sequence: chemical shift, multiplicity (s = singlet, d = doublet, t = triplet, q = quartet, br = broad, m = multiplet), coupling constants (Hz), and integration. ¹³C spectra were recorded at 125 MHz (at CSUCI) with complete proton decoupling; chemical shifts are listed to the nearest tenth of a ppm with the solvent resonance as the internal standard (CDCl₃ δ 77.16; (CD₃)₂CO δ 29.84, (CD₃)₂SO δ 40.45). High-resolution mass spectra (HRMS) were recorded at University of Illinois (Urbana-Champaign, IL) using ESI-TOF methods. Elemental analyses were performed by Robertson Microlit Laboratories (Ledgewood, NJ).

Materials. 2-Amino-6-bromonaphthalene (Oakwood), sodium carbonate, potassium carbonate, tris(dibenzylideneacetone)dipalladium(0) ($\text{Pd}_2(\text{dba})_3$, Strem), 2-dicyclohexylphosphino-2',6'-dimethoxybiphenyl (SPhos, Aldrich), 4-pyridine boronic acid (Aldrich), silver(I) nitrate, petroleum ether, hexane, dichloromethane, ethyl acetate, 1,2-dichloro-ethane, glacial acetic acid, methanol, toluene, heptane, and chloroform were purchased and used without further purification. Dimethylformamide (DMF) was filtered through a short pad of alumina and then vacuum distilled over calcium hydride. Ethyl alcohol was distilled over calcium hydride and stored over 3 Å molecular sieves. Acetonitrile was dispensed from a Glass Contour solvent system built by Pure Process Technologies (Nashua, NH). Iodomethane was distilled over brass wool to a colorless oil and used immediately without storage.



6-Bromo-*N,N*-dimethylnaphthalene-2-amine (1). A 24/40, 250 mL round bottom flask containing a magnetic stir bar was charged with 4.24 g of 2-amino-6-bromonaphthalene (19.1 mmol, 1.0 equiv) and 5.26 g of potassium carbonate (38.1 mmol, 2.0 equiv) directly as purchased solids. The flask was equipped with a reflux condenser, evacuated, and purged with nitrogen on a Schlenk line. With stirring at room temperature, dimethylformamide (76.4 mL, 0.25 M) and iodomethane (3.0 mL, 48.1 mmol, 2.5 equiv) were then added by syringe under a positive pressure of argon. The base did not completely dissolve, resulting in a murky brown suspension. The reaction mixture was submerged in an oil bath at 60 °C and allowed to stir heated for 24 h, at which point TLC analysis confirmed the absence of starting material and smooth conversion to two products (desired **1** $R_f = 0.54$, monomethyl $R_f = 0.31$ in 3:1 petroleum ether : ethyl acetate). After cooling the flask to ambient temperature, the mixture was diluted with 50 mL of ethyl acetate and 25 mL of petroleum ether and transferred to a 250 mL separatory funnel. Upon subsequent addition of 100 mL of water, a bilayer was established with the top layer separating as a dark brown solution. The organic layer was collected, and the aqueous layer was washed with two additional 50 mL portions of 2:1 ethyl acetate : petroleum ether. The pooled organic layers were washed three times with equal volumes of saturated (aq.) sodium chloride to remove residual dimethylformamide from the extract. Purification by column chromatography with 9:1 petroleum ether : ethyl acetate as eluant gave substantial product but also 1.6 g of recovered secondary amine (monomethylated). This material was thus resubjected to the reaction conditions, this time with only 1.5 equiv of the electrophile. An analogous workup gave additional product that was also

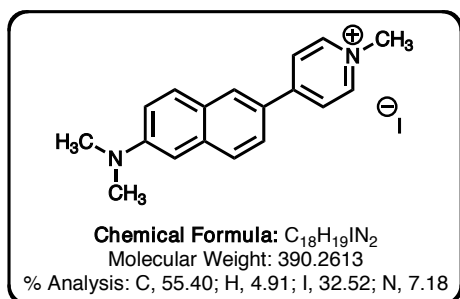
purified with a flash column. Solvent removal from the pure fractions through rotary evaporation resulted in spontaneous precipitation of an off-white, flaky solid (at low volumes) in spite of the supernatant being light orange in color. Before concentration to dryness, which routinely afforded a less pure, orange tacky solid, the free-flowing crystals were recovered by vacuum filtration on a medium porosity glass frit and washed briefly with ice-cold petroleum ether. Isolation and further drying under high vacuum furnished 4.06 g of product in two crops as a white flaky solid (85% yield). A scale-up reaction carried out using nominally the same procedure produced 8.4 g **1** in 55% yield. Melting point = 122–124 °C. IR (KBr pellet): 2884 (m), 1625 (s), 1589 (s), 1559 (w), 1505 (s), 1382 (s), 1236 (m), 1181 (m), 1159 (m), 1060 (m), 937 (m), 877 (m), 844 (s), 807 (s). ¹H NMR (500 MHz, CDCl₃): δ 7.83 (s, 1H), 7.61 (d, *J* = 8.8 Hz, 1H), 7.52 (d, *J* = 8.8 Hz, 1H), 7.42 (dd, *J* = 8.8, 1.5 Hz, 1H), 7.17 (dd, *J* = 9.3, 2.2 Hz, 1H), 6.87 (d, *J* = 1.5 Hz, 1H), 3.05 (s, 6H). ¹³C NMR (125 MHz, CDCl₃): δ 149.7, 148.9, 133.6, 129.5, 127.97, 127.94, 127.9, 117.2, 115.2, 106.2, 40.8. HRMS Calcd for C₁₂H₁₃BrN⁺ (M+1): 250.0231. Found: 250.0233. Anal Calcd for C₁₂H₁₂BrN: C, 57.62; H, 4.84. Found: C, 57.72; H, 4.61.



***N,N*-Dimethyl-6-(pyridine-4-yl)naphthalene-2-amine (3).** A heavy-walled glass pressure vessel equipped with a magnetic stir bar and a threaded Teflon/O-ring seal was charged with 6-bromo-*N,N*-dimethylnaphthalene-2-amine (**1**, 967 mg, 3.87 mmol, 1.0 equiv), 4-pyridine boronic acid (**2**, 715 mg, 5.82 mmol, 1.5 equiv), sodium carbonate (820 mg, 7.74 mmol, 2.0 equiv),

tris(dibenzylideneacetone)dipalladium(0) (53 mg, 0.058 mmol, 0.015 equiv), and SPhos (95 mg, 0.23 mmol, 0.060 equiv). The vessel was then fitted with a rubber septum and a vent needle, evacuated, and purged with argon on a Schlenk line. Anhydrous dimethylformamide (62.0 mL) and ethanol (15.5 mL) were introduced by syringe under a positive pressure of argon (4:1 DMF–EtOH, 0.05 M). Some of the solid reaction contents dissolved, but homogeneity was not achieved at ambient temperature; a murky light green suspension was observed. After removing the rubber septum and sealing the reactor, the mixture was stirred vigorously for 4 h at 85 °C (oil bath). At this point, the reaction mixture was less turbid and a Pd black precipitate was visible. A routine TLC analysis confirmed the absence of the starting bromoarene (**1**). The reaction mixture was cooled to room temperature, transferred to a separatory funnel, and diluted with water (75 mL) and ethyl acetate (75 mL). After removing the organic layer, the aqueous layer was washed two times

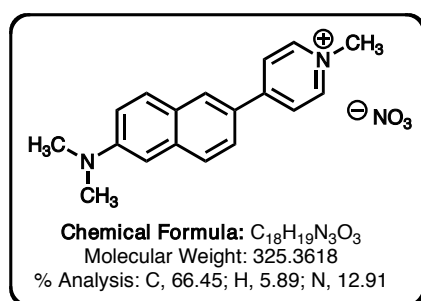
with 50 mL of ethyl acetate, and the combined organic layers were washed three times with an equal volume of saturated sodium chloride in order to remove residual dimethylformamide. The purified extract was dried over MgSO_4 , filtered through a medium porosity glass frit, and concentrated by rotary evaporation to give a bright yellow, solid residue. The crude material was purified by recrystallization from hot toluene. In the event, ~1 gram of the crude solid dissolved readily in 35-40 mL of boiling toluene but required a hot filtration in order to remove traces of insoluble deposits. Slow cooling of the hot filtrate delivered the product as yellow nodules and clusters. After leaving the flask at $-20\text{ }^\circ\text{C}$ overnight to complete precipitation, crystals were isolated on a medium porosity glass frit, washed with small portions of cold petroleum ether, and dried under high vacuum. These operations furnished 614 mg (64% yield) of product as a microcrystalline, canary yellow solid. Additional pure material was recovered by dry-packing the mother liquor onto silica gel and eluting over a 4 cm wide x 10 cm long column with 1:1:1 petroleum ether : ethyl acetate : CH_2Cl_2 (dichloromethane additive helps prevent 'streaking' of the diamine, $R_f = 0.35$). The chromatography serves to remove uncharacterized non-polar impurities ($R_f > 0.50$) and 4,4'-bipyridine ($R_f = 0.15$) derived from homocoupling of 4-pyridine boronic acid (**2**). Concentration of the desired fractions gave an additional 270 mg of product as a yellow solid, making the total yield to 92%. A scale-up reaction carried out using nominally the same procedure produced 4.1 g **3** in 49% yield. Melting point = 226–228 $^\circ\text{C}$. IR (KBr pellet): 2918 (w), 2896 (w), 1616 (s), 1603 (s), 1592 (s), 1541 (m), 1506 (s), 1447 (w), 1425 (w), 1412 (w), 1383 (s), 1354 (m), 1340 (m), 1225 (m), 1190 (w), 1176 (w), 1144 (w), 1066 (w), 991 (m), 829 (w), 808 (w), 796 (w). ^1H NMR (500 MHz, CDCl_3): δ 8.65 (dd, $J = 4.9, 1.5$ Hz, 2H), 8.03 (d, $J = 1.5$ Hz, 1H), 7.77 (dd, $J = 18.6, 9.3$ Hz, 2H), 7.75-7.73 (m, 2H), 7.67 (dd, $J = 8.3, 2.0$ Hz, 1H), 7.21 (dd, $J = 9.3, 2.5$ Hz, 1H), 6.92 (d, $J = 2.5$ Hz, 1H), 3.11 (s, 6H). ^{13}C NMR (125 MHz, CDCl_3): δ 154.7, 149.7, 147.8, 142.1, 131.6, 129.8, 127.4, 126.9, 124.6, 121.8, 117.0, 105.7, 99.4, 40.8. HRMS Calcd for $\text{C}_{17}\text{H}_{17}\text{N}_2^+$ (M+1): 249.1392. Found: 249.1391. Anal Calcd for $\text{C}_{17}\text{H}_{16}\text{N}_2$: C, 82.22; H, 6.49; N, 11.28. Found: C, 81.39; H, 6.41; N 11.11.



4-(6-(Dimethylamino)naphthalen-2-yl)-1-methylpyridinium iodide (DANPY⁺I⁻, 4).

In a dry glass vial containing a magnetic stir bar and a Teflon-lined screw cap, 200 mg of *N,N*-dimethyl-6-(pyridine-4-yl)-naphthalene-2-amine (**3**, 0.81 mmol) was dissolved in 16 mL of dry acetonitrile (0.05 M) under argon. To the resulting light yellow solution, iodomethane (75 μ L, 1.2 mmol, 1.5 equiv) was added by gas-tight syringe. The vial was capped and placed in an oil bath heated to 60 °C. After 10 min, the solution was bright orange in color and a gentle reflux of solvent had begun. After 24 h of stirring at this temperature, a bright orange solution with a dark red precipitate was observed. The solid is the corresponding pyridinium iodide and can be recovered in low yield (by microfiltration). Typically, the mixture was cooled to room temperature and homogenized using a small amount of commercial chloroform (which contains 2–3% ethanol). Glacial acetic acid (50 μ L, 0.87 mmol, 1.1 equiv) was also added to ensure an acidic pH and promote homogeneity. The solution was then saturated with silica gel, dry-packed onto the adsorbent, and filtered through a broad but short plug of silica (4 cm wide x 4 cm long) with 87:10:3 dichloroethane : methanol : acetic acid as eluant ($R_f = 0.30$). An uncharacterized yellow-orange fraction elutes just before the desired product, which is bright red in solution and light blue to violet under long wave UV irradiation. The column also serves to remove dicationic impurities, since the dimethylaniline domain can quaternize by methylation or simple protonation. Pooling and rinsing of pure fractions with chloroform, followed by concentration on a rotovap connected to a high vacuum delivered a bright red solid residue. Prolonged exposure to a high vacuum may be necessary to remove the less volatile acetic acid. The tacky solid residue was then recrystallized from a boiling mixture of chloroform (40 mL) and methanol (3-5 mL, just enough to promote dissolution) using a hot filtration step to remove any insoluble material. Upon slow cooling to 23 °C and further cooling to -20 °C overnight, the dye deposited as thin, orange needles that were collected on a fine porosity glass frit, washed twice with petroleum ether, and dried under high vacuum. By this method, 197 mg (78% yield) of product was recovered in a single crop. Another option, ideal for smaller amounts of the dye or second crops, is to layer a saturated chloroform-methanol (~10:1) solution with an excess of heptane. By slow diffusion of the hydrocarbon, fine needles are obtained and isolated as above. A scale-up reaction carried out using nominally the same procedure produced 2.6 g **4** in 48% yield. Melting

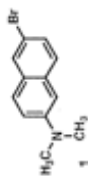
point = 250 °C (decomposition). IR (KBr pellet): 3448 (br, s), 1618 (s), 1560 (s), 1508 (m), 1385 (s), 1229 (w), 1190 (w), 835 (m), 669 (m). ¹H NMR (500 MHz, (CD₃)₂CO): δ 9.06 (d, *J* = 6.8 Hz, 2H), 8.60 (d, *J* = 6.8 Hz, 2H), 7.99 (dd, *J* = 8.8, 2.0 Hz, 1H), 7.94 (d, *J* = 9.3 Hz, 1H), 7.86 (d, *J* = 8.8 Hz, 1H), 7.34 (dd, *J* = 9.3, 2.0 Hz, 1H), 7.05 (d, *J* = 2.4 Hz, 1H), 4.57 (s, 3H), 3.15 (s, 6H). ¹³C NMR (75 MHz, (CD₃)₂SO): δ 55.0, 151.0, 145.9, 137.5, 131.3, 129.8 (d, *J*_{CN} = 8.9 Hz), 128.0, 126.3, 126.1, 125.0, 123.5, 117.7 (d, *J*_{CN} = 8.8 Hz), 105.5 (d, *J*_{CN} = 17.7 Hz), 47.5 (d, *J*_{CN} = 17.6 Hz), 40.8. HRMS Calcd for C₁₈H₁₉N₂⁺: 263.1549. Found: 263.1548. Anal Calcd for C₁₈H₁₉IN₂: C, 55.40; H, 4.91; N, 7.18. Found: C, 55.30; H, 4.92; N, 7.02.



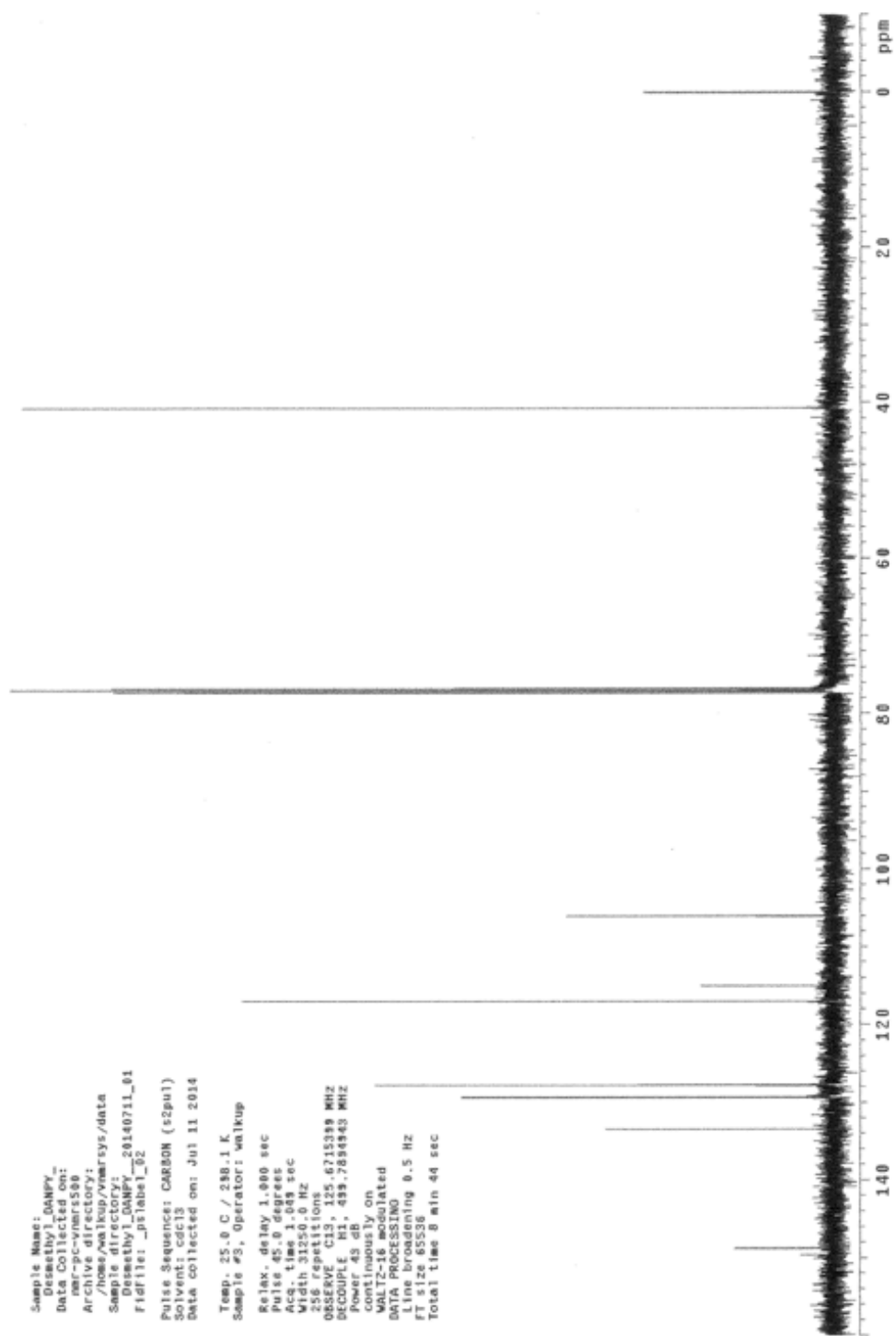
4-(6-(Dimethylamino)naphthalen-2-yl)-1-methyl-pyridinium nitrate (DANPY⁺NO₃⁻, **5).** In a vial containing a magnetic stir bar and a Teflon-lined screw cap, 36.1 mg of **DANPY⁺I⁻** (0.0925 mmol) was suspended in 3.0 mL of dry acetonitrile (0.025 M) under argon. The starting dye appeared to dissolve, giving way to a bright orange yet turbid solution. In

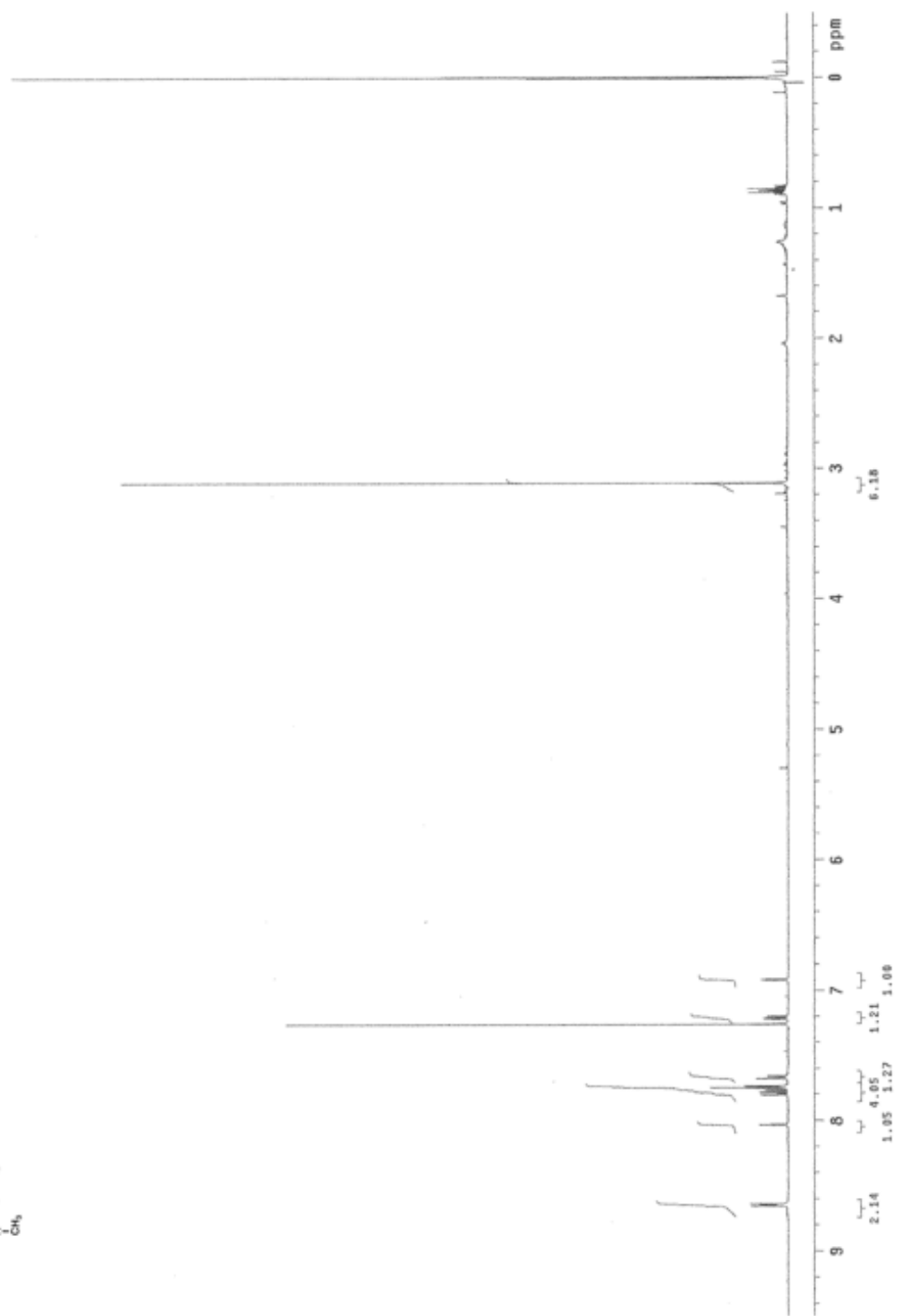
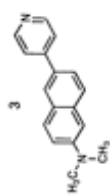
a separate dry vial, a solution of 16.5 mg of silver(I) nitrate (0.0971 mmol, 1.05 equiv) in 0.6 mL of acetonitrile was prepared. The light yellow salt solution was then added to the reaction dropwise from a syringe with magnetic stirring, causing immediate precipitation of a very fine, light yellow powder (presumed to be silver(I) iodide). The heterogeneous mixture was stirred for an additional 2 hours at 23 °C, but no further color changes were observed. The precipitate was separated from the bright orange supernatant by filtration through a plug of cotton in a Pasteur pipette, using a small portion of acetonitrile to rinse the vial. Solvent removal under reduced pressure afforded 30.1 mg (quantitative) of an orange solid (**5**) that was indistinguishable from **DANPY⁺I⁻** by ¹H NMR or FT-IR spectroscopy. Melting point = 250 °C (decomposition). HRMS Calcd for C₁₈H₁₉N₂⁺: 263.1555. Found: 263.1548.

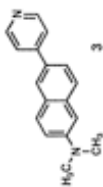
NMR Spectra:



Sample Name: Desmethy1_04NPFY
 Data Collected on: nmr-pc-vnars588
 Archive directory: /home/walkup/vnarsys/data
 Sample directory: Desmethy1_04NPFY_20140711_01
 Fidfile: _pftlabel_02
 Pulse Sequence: CARBON (s2pu1)
 Solvent: cdcl3
 Data collected on: Jul 11 2014
 Temp: 25.0 C / 288.1 K
 Sample #5, operator: walkup
 Relax. delay 1.000 sec
 Pulse 45.0 degrees
 Acq. time 1.049 sec
 Width 31250.0 Hz
 Resolution 0.100 Hz
 OBSERVE CH3 125.6715389 MHz
 DECOUPLE H1 499.7844443 MHz
 Power 49 dB
 continuously on
 WALTZ-16 modulated
 DATA PROCESSING
 Line broadening 0.5 Hz
 FT size 65536
 Total time 8 min 44 sec







Sample Name:

Data Collected on:
 nmr-pc-v0615500
 Archive directory:

Sample directory:

Fidfile: CARBON

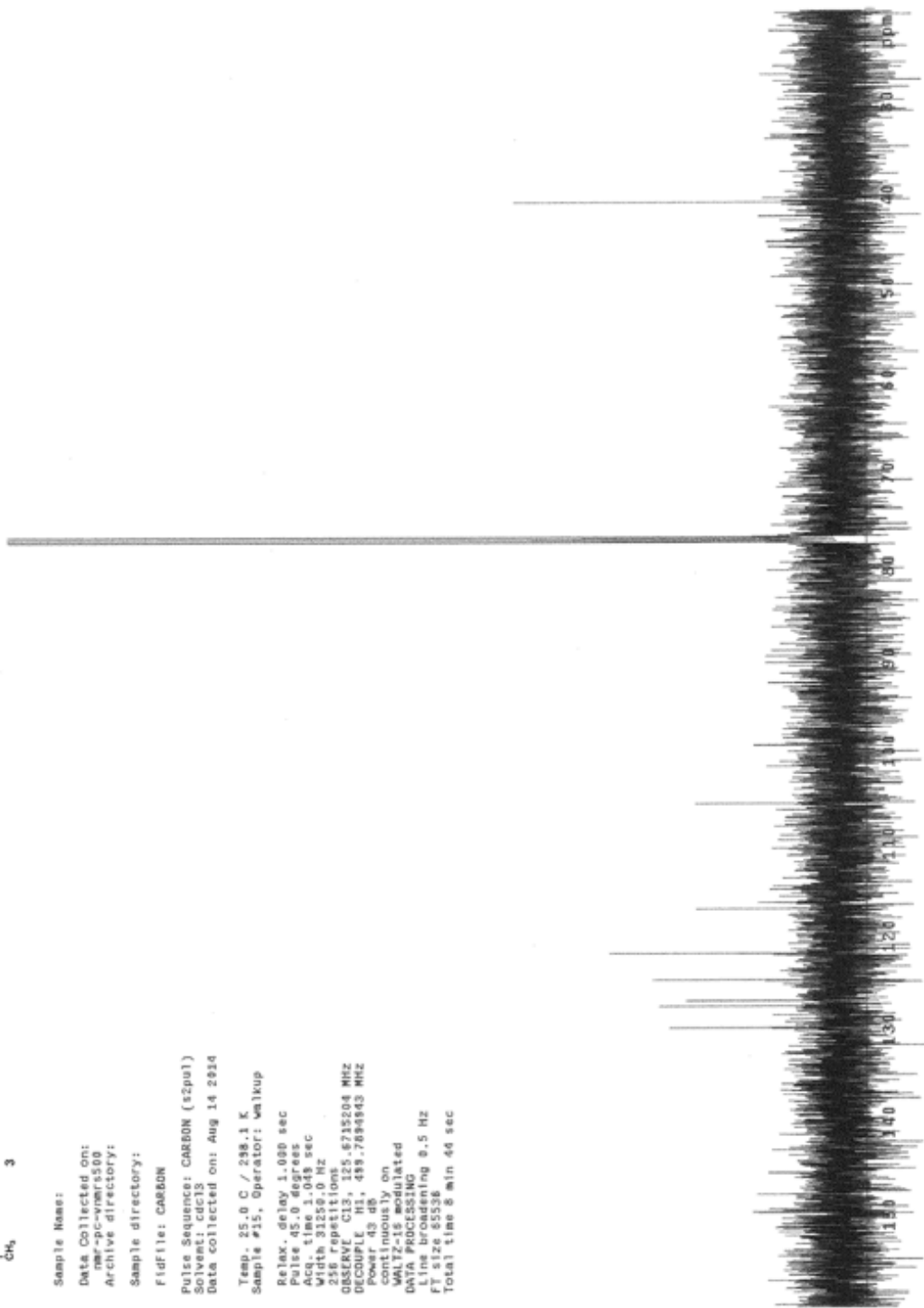
Pulse Sequence: CARBON (szpul)
 Data collected on: Aug 14 2014

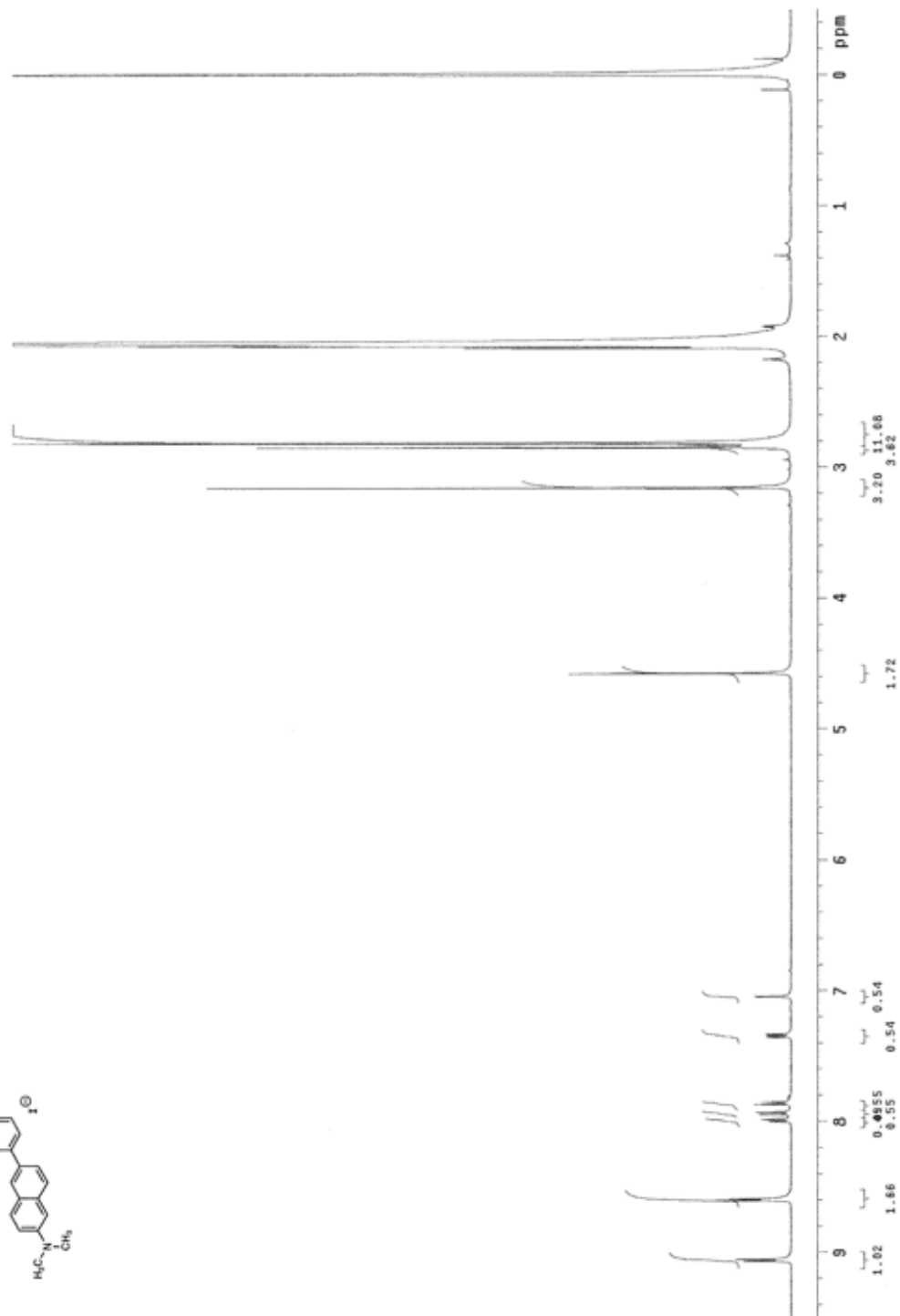
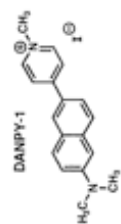
Temp. 35.0 C / 298.1 K
 Sample #15, Operator: Walkup

Relax. delay 1.000 sec
 Pulse 45.0 degrees
 Acq. time 1.048 sec
 Width 31250.0 Hz

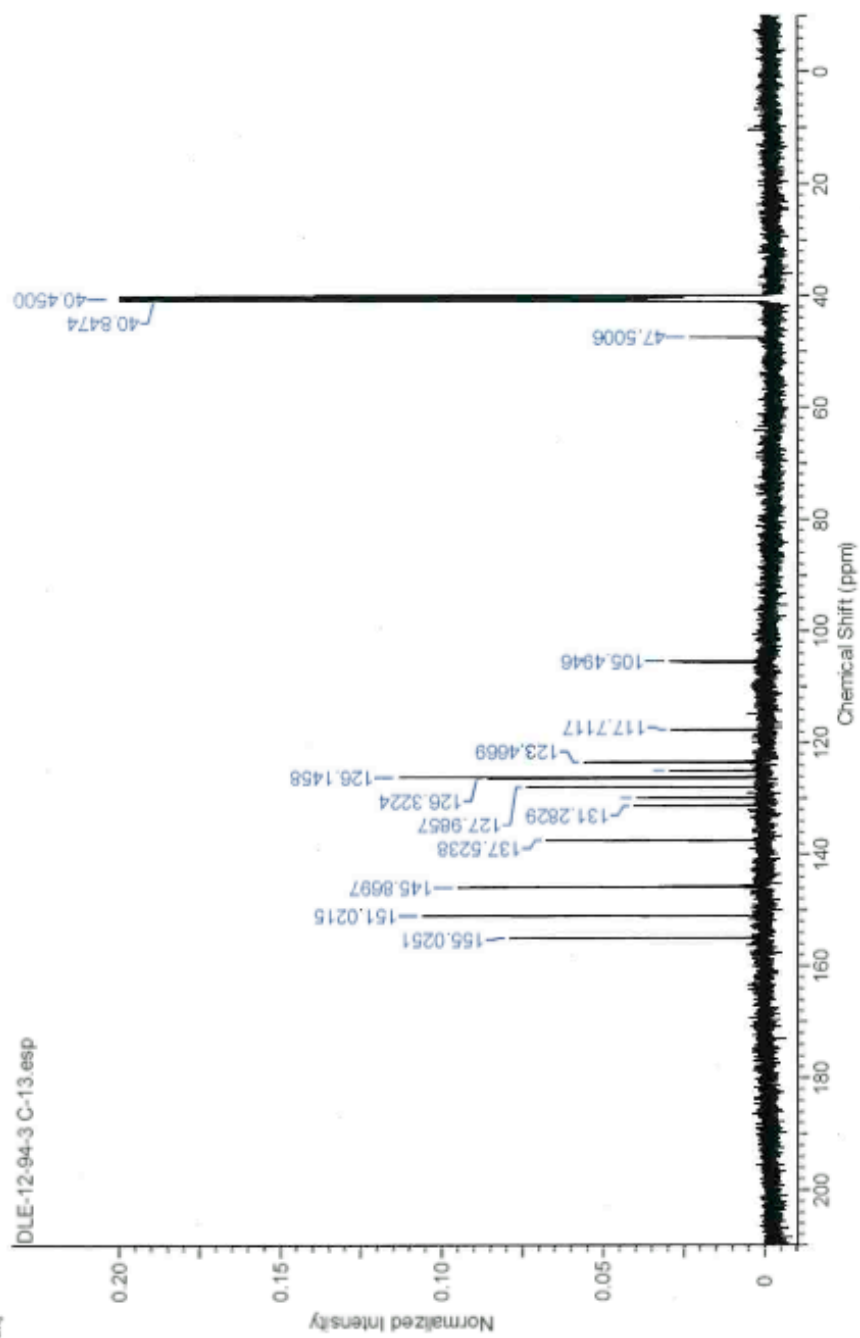
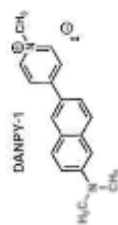
256 repetitions
 OBSERVE: C13, 125.5715204 MHz
 PULPROG: zgpg30
 Power 43 db

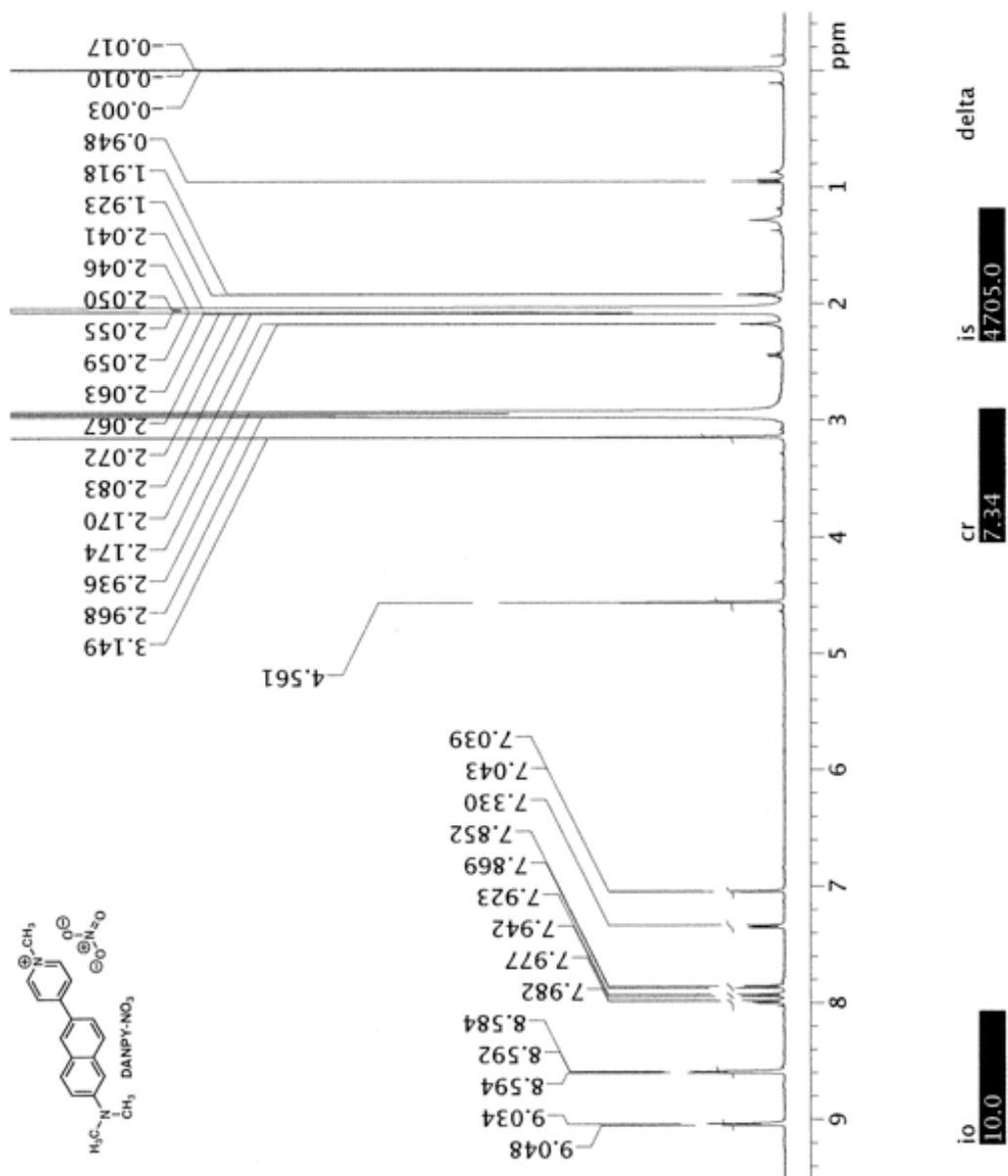
continuously on
 WALTZ-16 modulated
 DATA PROCESSING
 Line broadening 0.5 Hz
 FT size 85536
 Total time 8 min 46 sec





¹³C NMR of DANPY-1
(in DMSO-d₆)
sample # DLE-12-94-3





Infrared and Raman spectra:

Solid-phase IR and Raman spectra were recorded for DANPY-1 in advance of 2013 sum-frequency generation (SFG) experiments¹ conducted at the University of Cambridge. The infrared spectrum was recorded using a Perkin Elmer Spectrum 100 IR spectrometer with a liquid nitrogen cooled MCT detector and a horizontal ATR attachment with a germanium substrate; DANPY-1 was cast on the substrate from methanol solution. The Raman spectrum was recorded for a sample of DANPY-1 powder using an Ocean Optics QE 65 Pro spectrometer with a 785 nm source (Frequency-stabilized 500 mW CNI fiber coupled laser) and baseline subtracted using a broad-band Savitzky-Golay filter in Matlab. Computational spectra were calculated at the B3LYP/cc-pVTZ level of theory in PCM methanol. Intensities and peak widths are not directly comparable between the computed and experimental spectra as they were determined in different phases and the computational spectra lack any effects from counterions or residual solvent.

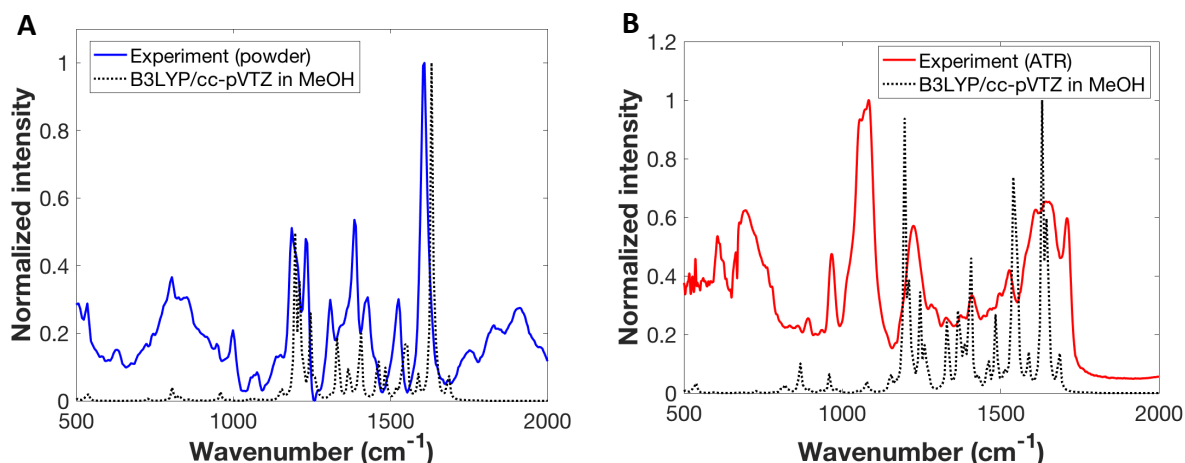


Figure S1. Solid-phase infrared (A) and Raman (B) spectra of DANPY-1 overlaid with solution-phase DFT (B3LYP/cc-pVTZ) predictions.

Identity and variation of counterion:

The counterion for DANPY-1 had initially been reported²⁻³ as acetate based on ¹H and ¹³C NMR due to the presence of a stoichiometric quantity (expected O fraction of 9.92 %) of acetic acid from the final reaction step in the original 2011 batch of the dye. As acetate was not observed in NMR spectra from later batches, including those synthesized for this paper, elemental analysis (Galbraith Microlabs) was performed on the 2011 batch and confirmed that both iodine and an amount of oxygen corresponding the previously identified acetate/acetic acid were present (40.36 % I, 9.64% O). As 35.2% iodine would be expected for DANPY-1 and elevated iodine was not

observed for other batches, the excess likely represents the formation of triiodide (I_3^-), which was observed by crystallography (Figure 2 in main text) on a slightly less polar fraction obtained from chromatographic purification. The only experiments discussed in this manuscript that used material from the 2011 batch were the hyper-Rayleigh scattering (HRS) measurements; as these experiments are complex, HRS data was re-scaled to reflect the impurity fraction (negligible expected hyperpolarizability).

Crystallography:

A brown needle, measuring $0.60 \times 0.03 \times 0.02 \text{ mm}^3$ was mounted on a loop with oil. Data was collected at 90 K on a Bruker APEX II single crystal X-ray diffractometer, Mo-radiation.

Crystal-to-detector distance was 40 mm and exposure time was 10 seconds per frame for all sets. The scan width was 0.5° . Data collection was 100 % complete to 25° in θ . A total of 198409 reflections, merged to 39746 reflections with separate Friedel pairs were collected covering the indices, $h = -37$ to 37 , $k = -18$ to 18 , $l = -27$ to 27 . 19882 reflections were symmetry independent and the $R_{\text{int}} = 0.0384$ indicated that the data was of excellent quality (0.07). Indexing and unit cell refinement indicated a primitive monoclinic lattice. The space group was found to be $P 2_1/n$ (No.14).

The data was integrated and scaled using SAINT, SADABS within the APEX2 software package by Bruker.⁴

Solution by direct methods (SHELXS, SIR97⁵) produced a complete heavy atom phasing model consistent with the proposed structure. The structure was completed by difference Fourier synthesis with SHELXL97.⁶⁻⁷ Scattering factors are from Waasmair and Kirfel.⁸ Hydrogen atoms were placed in geometrically idealised positions and constrained to ride on their parent atoms with C---H distances in the range 0.95-1.00 Angstrom. Isotropic thermal parameters U_{eq} were fixed such that they were $1.2U_{\text{eq}}$ of their parent atom U_{eq} for CH's and $1.5U_{\text{eq}}$ of their parent atom U_{eq} in case of methyl groups. All non-hydrogen atoms were refined anisotropically by full-matrix least-squares.

Table S1 summarizes the data collection details. Figure 2 (main manuscript) shows an ORTEP⁹ of the asymmetric unit.

Table S1. Crystallographic data for DANPY-1 with triiodide counterion

Empirical formula	C ₁₈ H ₁₉ I ₃ N ₂	
Formula weight	644.05	
Temperature	90(2) K	
Wavelength	0.71073 Å	
Crystal system	Monoclinic	
Space group	P 2 ₁ /n	
Unit cell dimensions	a = 28.113(3) Å	α = 90°.
	b = 13.9070(15) Å	β = 94.807(5)°.
	c = 20.473(2) Å	γ = 90°.
Volume	7976.3(16) Å ³	
Z	16	
Density (calculated)	2.145 Mg/m ³	
Absorption coefficient	4.704 mm ⁻¹	
F(000)	4800	
Crystal size	0.600 x 0.030 x 0.020 mm ³	
Theta range for data collection	1.454 to 28.466°.	
Index ranges	0 ≤ h ≤ 37, -18 ≤ k ≤ 18, -27 ≤ l ≤ 27	
Reflections collected merged	39746	
Independent reflections	19882 [R(int) = 0.0384]	
Completeness to theta = 25.000°	100.0 %	
Refinement method	Full-matrix least-squares on F ²	
Data / restraints / parameters	19882 / 36 / 842	
Goodness-of-fit on F ²	1.061	
Final R indices [I > 2σ(I)]	R1 = 0.0559, wR2 = 0.1324	
R indices (all data)	R1 = 0.1019, wR2 = 0.1481	
Largest diff. peak and hole	5.073 and -2.755 e.Å ⁻³	

During structure refinement, a noticeable improvement of statistical data was achieved with application of twin matrix (0 0 1, 0 1 0, -1 0 0), although the twin percentage of 0.00091 is vanishing small.

The asymmetric cell contains 4 independent DANPY-1 molecules in addition to 4 triiodides. The dye molecules are aligned closely parallel to the {0 1 0} faces of the crystals, while two triiodides are approximately parallel to the b-axis, the other two are approximately within planes parallel to (1 0 -1).

In addition to the crystallographic twofold screw axis along the b-axis, 93% of the atoms are related by a non-crystallographic b/2 glide plane which does not increase the symmetry or lead to a different space group as it is approximately established but it does create antiparallel pairs of

DANPY-1 molecules which reduces the static dipole of the anisotropic unit. The inversion of the space group counterbalances the remaining static dipole.

Several van der Waals interactions connect the DANPY-1 dyes to the triiodides as summarized in Table S2.

Table S2. van der Waals interactions [\AA and $^\circ$].

D-H...A	d(D-H)	d(H...A)	d(D...A)	<(DHA)
C(5)-H(5)...I(8)#1	0.95	3.17	3.809(7)	126.3
C(6)-H(6)...I(7)#1	0.95	3.13	4.041(6)	161.2
C(6)-H(6)...I(8)#1	0.95	3.05	3.737(6)	130.4
C(13)-H(13)...I(10)#2	0.95	3.22	4.034(7)	144.3
C(17)-H(17A)...I(5)#3	0.98	3.24	3.819(7)	119.2
C(18)-H(18A)...I(10)#2	0.98	3.24	4.057(8)	141.5
C(20)-H(20)...I(3)#4	0.95	2.88	3.826(7)	171.6
C(23)-H(23)...I(11)#5	0.95	3.21	4.141(7)	166.5
C(24)-H(24)...I(7)	0.95	2.98	3.880(6)	159.1
C(31)-H(31)...I(9)#6	0.95	3.29	4.155(9)	152.2
C(36)-H(36B)...I(3)	0.98	3.29	4.053(7)	136.4
C(37)-H(37A)...I(9)#6	0.98	3.18	3.915(7)	132.9
C(38)-H(38)...I(10)#7	0.95	3.26	4.124(6)	151.8
C(39)-H(39)...I(9)#8	0.95	3.33	4.258(6)	167.6
C(41)-H(41)...I(5)#3	0.95	3.17	3.799(7)	125.6
C(42)-H(42)...I(5)#3	0.95	3.07	3.756(7)	130.0
C(42)-H(42)...I(6)#3	0.95	3.14	4.055(6)	161.8
C(49)-H(49)...I(4)#4	0.95	3.32	4.196(7)	154.3
C(55)-H(55B)...N(4)#8	0.98	2.67	3.646(9)	171.0
C(56)-H(56)...I(12)#9	0.95	2.92	3.860(7)	169.5
C(59)-H(59)...I(2)#10	0.95	3.20	4.131(6)	165.6
C(60)-H(60)...I(6)#8	0.95	2.98	3.897(6)	161.4
C(67)-H(67)...I(1)#11	0.95	3.22	4.025(7)	143.2
C(71)-H(71A)...I(8)#8	0.98	3.14	3.733(7)	120.5
C(71)-H(71C)...I(7)	0.98	3.22	4.032(8)	140.9
C(72)-H(72A)...I(1)#11	0.98	3.31	4.136(8)	143.7

Symmetry transformations used to generate equivalent atoms:

#1 $x-1, y, z$ #2 $-x+1, -y, -z+1$ #3 $-x+1/2, y-1/2, -z+1/2$
 #4 $x+1/2, -y+1/2, z+1/2$ #5 $-x+3/2, y+1/2, -z+1/2$
 #6 $x-1/2, -y+1/2, z-1/2$ #7 $x-1/2, -y-1/2, z-1/2$
 #8 $-x+3/2, y-1/2, -z+1/2$ #9 $-x+2, -y, -z+1$ #10 $x+1, y, z$
 #11 $-x+1, -y, -z$

Computational Methods:

All density functional theory (DFT) calculations for this paper were performed using Gaussian '09.¹⁰ Hyperpolarizability calculations were performed at the M062X/6-31+G(d) level of theory, which had previously been demonstrated to be effective for determination of relative hyperpolarizabilities.¹¹ IR/Raman calculations and rotational barrier calculations were performed at the B3LYP/cc-pVTZ level of theory due to the B3LYP functional's superior performance for vibrational spectroscopy.¹² Excited-state calculations were performed at the TD-M062X/6-31+G(d) level of theory. All calculations were performed using an IEF-PCM implicit solvent environment and default settings. All properties were calculated on optimized geometries that had been determined using the same method, basis, and implicit solvent. SCF calculations were converged to $< 10^{-10}$ au RMS error in the density matrix. Hyperpolarizabilities were calculated using analytic differentiation (coupled-perturbed Hartree-Fock/Kohn-Sham, CPHF) and default CPHF settings.

Dihedral and molecular orbital analysis:

The dimethylnaphthaleneamine donor and methylpyridinium acceptor in DANPY-1 are bridged with a single aryl-aryl bond, and the relative alignment of these moieties is a key determining factor for intramolecular charge transfer (ICT) excitation processes.¹³ High torsional flexibility also contributes to The rotational barrier for the dihedral angle between the naphthyl and pyridyl moieties in DANPY-1 was determined using DFT calculations and found to be 25 kJ/mol (6 kcal/mol) in a methanol implicit solvent environment and 28 kJ/mol in a chloroform implicit solvent environment. Relative energies as a function of dihedral angle are shown in the left-hand panel of Figure S2. The rotational barrier in methanol is nearly identical (< 1 kJ/mol difference) to that observed from calculations on Prodan using the same DFT functional.¹³ Given the size of the barrier, perpendicular orientation of the two aryl moieties is unlikely but that a coplanar orientation is thermally accessible with a difference between the lowest-energy geometry and planar structure of < 5 kJ/mol ($2 k_B T$ at 300 K), enabling stacking with other aromatic groups such as the π -system of nucleic acid bases. The influence of the aryl-aryl bond is further illustrated by examining the electronic structure of the molecule; orbital and differential density plots are shown in the right-hand panel of Figure S2. At the lowest-energy geometry, the HOMO is predominantly localized on the donor end of the molecule, and the LUMO is predominantly localized on the acceptor end of the molecule. The ICT nature of the first excitation is confirmed

by taking the difference in the total electron density between the first singlet excited state (S_1) and the ground state (S_0); electron density substantially decreases on the donor and increases on the acceptor when the chromophore is excited.

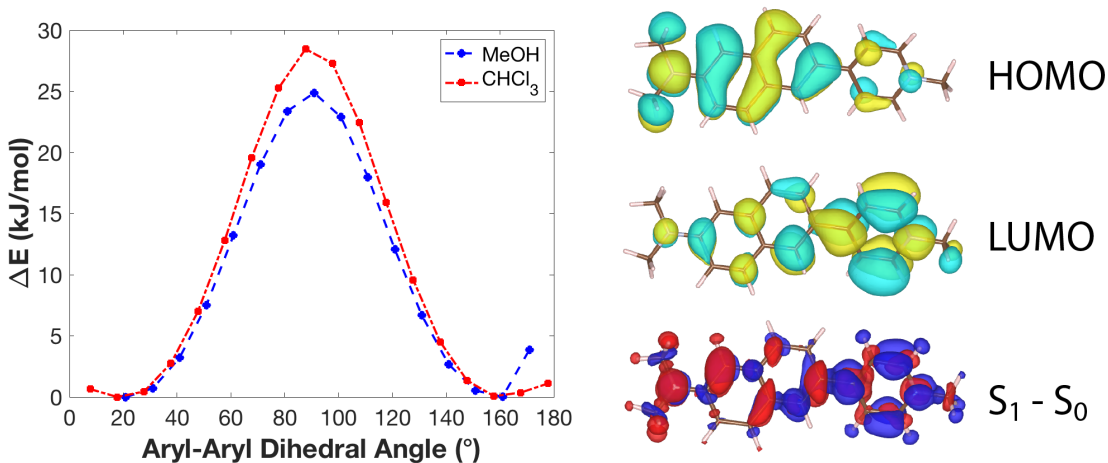


Figure S2. (left) DANPY pyridinium-naphthyl rotational barrier calculated at the B3LYP/cc-pVTZ level of theory in both methanol and in chloroform. (right) Frontier orbitals of DANPY-1 calculated at the M062X/6-31+G(d) level of theory in methanol, plus the S_0 - S_1 differential density. In the differential density plot, red represents loss of electron density and blue represents gain of electron density.

The large shift in electron density can also be observed by comparing the ground and excited state dipole moments (Table S3). DANPY-1 has a large (~ 15 D) dipole moment in the ground state, but a small and oppositely-oriented (170° angular difference) dipole moment in the S_1 state. Dipole reversal occurs due to transfer of charge to the pyridinium on excitation. The larger ground-state dipole in higher-polarity solvents and reduction in the dipole moment on charge transfer are consistent with a lower excitation energy (ΔE_{01}) in less polar environments.

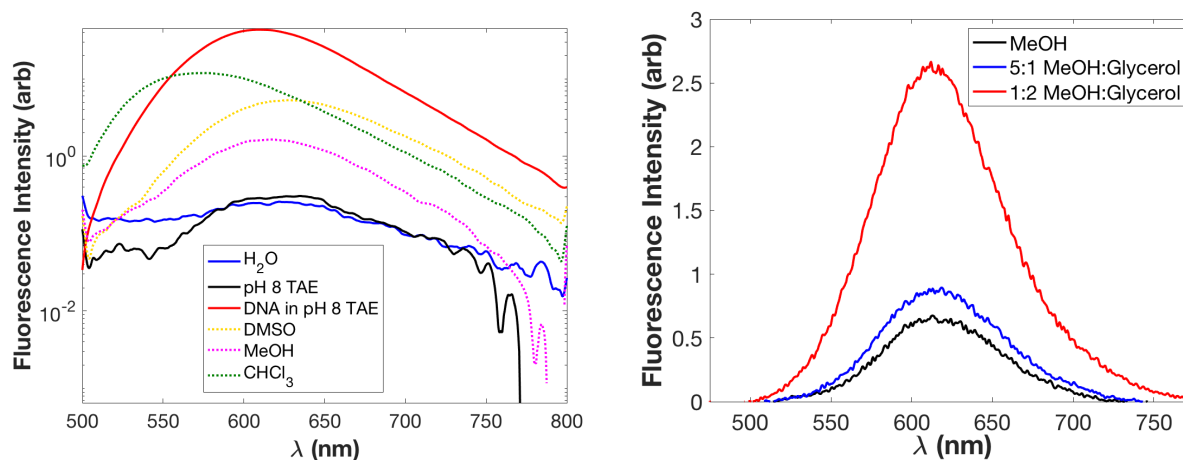
Table S3. Computed dipole moments for DANPY-1

Property	DANPY-1 in CHCl_3	DANPY-1 in MeOH
Ground-state dipole (μ_0) (D)	14.43	15.73
S_1 dipole (μ_1) (D)	2.41	2.56
Angle between μ_0 and μ_1 ($^\circ$)	170	169
$ \Delta\mu = \mu_1 - \mu_0 $ (D)	16.81	18.25
Transition dipole μ_{01} (D)	9.72	9.85
Angle between μ_0 and μ_{01} ($^\circ$)	8	9
ΔE_{01} (eV)	2.88	3.01

Absorbance and fluorescence methodology:

Absorbance measurements were recorded using a Shimadzu UV-1601 spectrophotometer in double-beam mode with a pure solvent blank. Fluorescence measurements were recorded with a Perkin-Elmer LS-50B fluorimeter using an excitation wavelength of 450 nm and a grating width of 15 nm for both excitation and emission. Rayleigh scattering contributions to the fluorescence signal within the wavelength range measured were negligible. Absorbance and fluorescence measurements were performed back-to-back (within 5 minutes of each other) for each sample. Fluorescence intensity of DANPY-1 in water and TAE buffer was much lower than in the other solutions and the traces are at baseline in Figure 3B in the main manuscript; data is plotted logarithmically in the left panel of Figure S3 to show the weak fluorescence response in these solutions.

An additional set of fluorescence measurements was also performed to assess the effects of viscosity on fluorescence intensity; these measurements used methanol:glycerol mixtures to vary viscosity while maintaining a nearly isodielectric environment. Measurements were recorded with a Perkins-Elmer LS50B fluorimeter using an excitation wavelength of 440 nm and a grating width of 10 nm for both excitation and emission; DANPY-1 concentration was 35 μM . Spectra are shown in the right-hand panel of Figure S3; a large increase in fluorescence intensity is observed in the more viscous glycerol mixtures than in pure methanol without any substantial shift in the wavelength of maximum emission. The integrated fluorescence intensity over absorbance at λ_{max} increases by a factor of 1.29 in 5:1 MeOH:Glycerol, and a factor of 3.17 in 1:2 MeOH:Glycerol.



Figures S3. (left) Fluorescence data from Figure 5B in the main text plotted on a logarithmic scale to show weak fluorescence of DANPY-1 in water or TAE buffer in the absence of DNA. **(right)**

Fluorescence lifetimes (τ_f) were determined by time-correlated single-photon counting using a PicoQuant PicoHarp 300 coupled with 405 nm diode laser driver. The experiment was performed using a pulse rate of 20 MHz, a 490 nm long-pass filter and a 50% neutral density filter, integrating for 15 minutes or until 25,000 counts were reached in a single bin (16 ps resolution). Solution concentrations ranged from 46.2 to 96.2 μM . The instrument response function (IRF) was determined using a scratched glass slide and had a FWHM of 0.228 ns. Data was deconvoluted and fit using DecayFit¹⁴ and a double-exponential model,

$$I(t) = a_1 e^{-t/\tau_1} + (1 - a_1) e^{-t/\tau_2} \quad (\text{S1})$$

χ^2 goodness-of-fit values ranged from 1.90 to 4.75, indicating reasonable fitting of the data. Despite the very small (< 0.005) weights for the second exponential, goodness-of-fit was improved by over an order of magnitude versus a single-exponential model. Lifetime curves are shown in Figure S4.

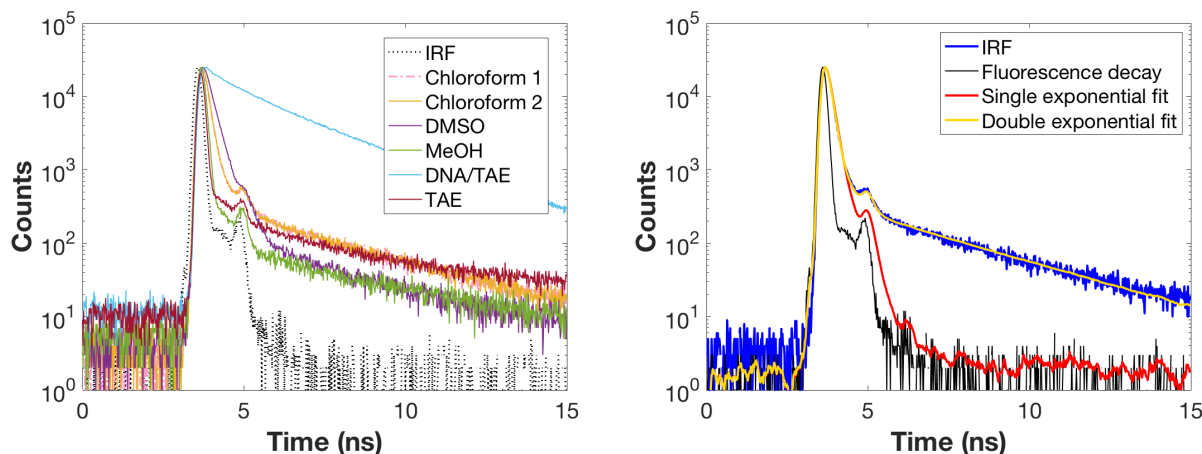


Figure S4. (left) Time-correlated single-photon counting curves for DANPY-1 in various solvents. A duplicate measurement was performed for chloroform to verify laser stability. (right) Single exponential ($\chi^2 = 52.96$) and double-exponential ($\chi^2 = 1.90$) fits for chloroform run 1.

Absolute fluorescence quantum yields (ϕ) were measured by the integrating sphere method using a Hamamatsu A10104-01 integrating sphere with an Hg/Xe source, excitation wavelength of 440 nm, 6 nm (FWHM) excitation bandwidth, and integration cutoff between incident light (excitation) and emission peaks of 475 nm. Two sets of measurements in different concentration ranges, one high (46.2 to 96.2 μM) and one low (1.61 to 3.52 μM) were performed

in order to ensure that results were not contaminated by self-quenching or self-absorbance. Results were reported for the low-concentration set, negligible difference was observed except for chloroform (0.043 at 56.0 μM vs. 0.068 at 1.61 μM). No low-concentration run was performed for TAE buffer due to minimal signal from the more concentrated (83.6 μM) sample. The quantum yield of reference dye fluorescein (129 μM , pH 11) was measured to be 0.792 using identical settings.

Two-photon cross-section measurement:

TPA cross-sections (δ) were measured via the TPEF method,¹⁵ referenced against 129 μM aqueous fluorescein at pH 11, ($\delta_r = 36 \text{ GM}$),¹⁶ and calculated using the methods described by De Meulenaere et al.,¹⁷ where the two-photon cross section of a sample,

$$\delta_s = \frac{C_r n_r F_s \phi_r}{C_s n_s F_r \phi_s} \quad (\text{S2})$$

where C is the concentration, n is the refractive index, F is the integrated intensity of the spectrum, and ϕ is the one-photon fluorescence quantum yield. Subscript r refers to reference and subscript s to sample, respectively.

Measurements were performed at the UW Molecular Analysis Facility using a Coherent Libra Ti:Sapphire laser at 800 nm for excitation and an Ocean Optics USB2000+ spectrometer for detection. The optical parametric amplifier (OPA) was bypassed such that excitation was performed directly with the fundamental. The pulse rate was 1 kHz, with a pulse duration (FWHM) was 56 fs. Spectra were integrated with a scan duration of 20 s, averaging 2 scans per spectrum. A minimum of three laser intensities were used per sample to verify the quadratic response to intensity characteristic of TPEF; laser intensities ranged from 2 mW to 34 mW. Cross-sections were calculated using data at 15 mW. Solution concentrations ranged from 1.61 to 3.52 μM . Integration time was reduced to 200 ms (averaging 10 scans) for the reference sample due to high intensity and integrated intensities were scaled accordingly. Integrated intensities F were calculated over the 475-725 nm range to minimize scattering contributions, after background subtraction. TPEF spectra for DANPY-1 are shown in Figure S6. No signal was obtained from the sample in TAE buffer. The data for methanol exhibits an anomalous lineshape compared to the other samples; integration yields $\delta = 440 \text{ GM}$, but this may be an artifact of low quantum yield and/or the lineshape.

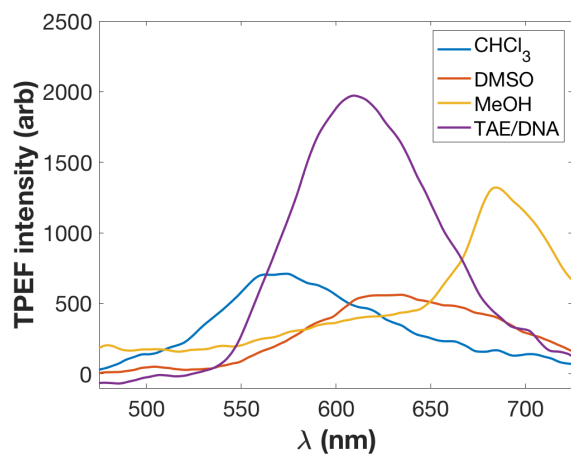
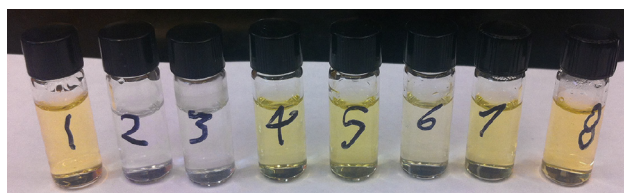
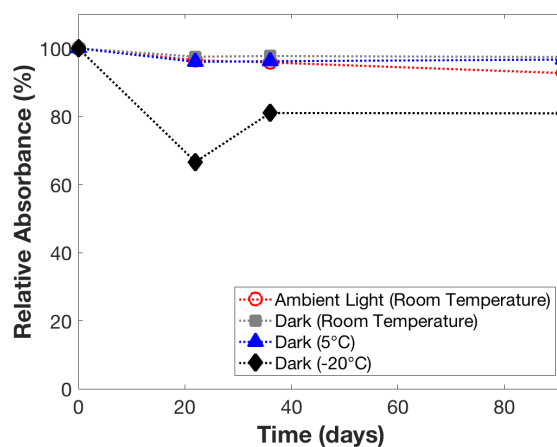


Figure S5. TPEF spectra for DANPY-1 after background subtraction and smoothing using the LOWESS method with a 5% (13 nm) window.

Photochemical stability:

We studied the long-term stability of 60 μM DANPY-1 solutions in TAE buffer under four different storage conditions: room temperature and ambient light, room temperature and dark, 5 $^{\circ}\text{C}$ and dark, or -20°C (frozen) and dark. The UV/Vis absorbance intensity at λ_{max} of the solutions was monitored periodically over 91 days (Figure S5, top). The best storage conditions were room temperature and dark, and 5 $^{\circ}\text{C}$ and dark, showing only a 2.6-3.3% decrease over 90 days. Storage at room temperature in ambient light and at -20°C in the dark resulted in decreases of 7.3% and 19%, respectively. The larger decrease for the -20°C sample was attributed to precipitation or decomposition from repeated freeze/thaw cycles. Samples were retained after the additional photostability study; the ambient light/room temperature samples were re-measured shortly prior to submission of a revised manuscript (1177 days). Fitting the original data to a single-exponential model yielded a photobleaching half-life of 792 ± 100 days (95% confidence), which was consistent with a fit including the extended data (846 ± 70 days). This suggests that the 90-day photostability study was sufficient to predict long-time behavior and that DANPY solutions should remain viable for several months if properly stored.

We also qualitatively assessed chemical stability (Figure S5, bottom) via exposure to oxidizing (NaClO), reducing (NaS_2O_3), acidic (HCl , $\text{B}(\text{OH})_3$), basic (NaOH), and de-aminating (NaNO_2) environments, with pH 7.2 TE (tris-EDTA) buffer and saturated NaCl as controls. After two weeks, only the strong Bronsted acid HCl , common bleaching agent NaClO , and de-aminating agent NaNO_2 (which is often used for destruction of ethidium bromide)¹⁸ caused any significant bleaching.



Control HCl NaClO NaOH Na₂S₂O₃ NaNO₂ NaCl B(OH)₃

Figure S6. (top) Long-term photochemical stability of DANPY-1 in pH 8 TAE buffer under four storage conditions as measured by absorbance at λ_{max} : RT and ambient light (blue); RT and dark (red); 5 °C and dark (yellow); and –20 °C and dark (purple). **(bottom)** Chemical stability of DANPY-1 after 14 days (vials 1-7) or 10 days (vial 8) of exposure to common laboratory reagents. (1) pH 7.2 TE buffer (control), (2) Household bleach (5% NaClO), (3) 1M HCl, (4) 6M NaOH, (5) Na₂S₂O₃, (6) NaNO₂, (7) NaCl, (8) B(OH)₃. Qualitative bleaching was observed for household bleach, HCl, and NaNO₂, but not for the other reagents.

DNA binding model/fitting:

DNA binding experiments used either a 2.5 or 3.0 mL aliquot of the dye solution, with 450-480 μL of 1.71 mM DNA solution added in 30 μL aliquots. DNA solutions were prepared using salmon sperm DNA from Sigma Aldrich, which was used as received. Solutions were prepared the day before use, thoroughly mixed, and allowed to sit overnight to settle and ensure complete dissolution of the DNA. Binding was monitored using a temperature-controlled Ocean Optics USB4000 diode array spectrophotometer with both the tungsten and D₂ bulbs enabled and

the integration settings tuned to maximize the instrument's dynamic range. Spectra were measured using 1 cm fused quartz cuvettes. The temperature controller and bulbs were allowed to equilibrate for > 1 hour before starting the experiment, and the instrument was baselined against pure buffer. Samples were mixed *in situ* using a magnetic stirrer, allowing at least 30 seconds for mixing before measuring spectra. The stirrer was briefly paused prior to recording each spectrum to prevent obstruction of the optical path by the stir bar.

Binding was analyzed by fitting to an identical/independent site binding model, in which free dye and sites on the DNA reversibly form a complex,

$$K = \frac{[LN]}{[L][N]} \quad (\text{S3})$$

where $[L]$ is the concentration of the ligand (dye), $[N]$ is the concentration of available base pairs (nucleotides) in the nucleic acid, $[LN]$ is the concentration of bound dye, and K is the binding (equilibrium) constant for the interaction. Since any given site or dye molecule is either bound or not, the total amount of material at any given point in the titration is conserved,

$$\begin{aligned} [L_0] &= [L] + [LN] \\ [N_0] &= [N] + [LN] \end{aligned} \quad (\text{S4})$$

In the context of a titration in which DNA is added to dye, these equations of mass balance can be rewritten as

$$\begin{aligned} [L_0] &= \frac{[L_0]_0 \cdot V_0}{V_0 + aV_{add}} \\ [N_0] &= \frac{[N_{add}] \cdot V_{add}}{V_0 + aV_{add}} \end{aligned} \quad (\text{S5})$$

Here, V_0 is the initial volume of the sample, $[L_0]_0$ is the concentration of dye before any DNA solution is added, V_0 is the initial volume of the dye sample, V_{add} is the volume of each aliquot of DNA added, and a is the number of aliquots added.

Obtaining the equilibrium constant requires determination of one of $[L]$, $[LN]$, or $[N]$, which enables calculation of the other quantities by way of the mass balance relations specified in Equation S4. These equations can be rewritten in terms of the fraction of bound ligand,

$$f_b = \frac{[LN]}{[L_0]} = \frac{[LN]}{[L] + [LN]} \quad (\text{S6})$$

The fraction of bound ligand can be determined by absorbance spectroscopy. If the absorbance of the ligand is monitored as DNA is added, then the total absorbance can be written as a sum of the absorbances of the free and bound ligands

$$A = f_b A_b + (1 - f_b) A_f \quad (\text{S7})$$

The absorbance can be related to concentration via the Beer-Lambert law, $A = \epsilon c l$, where c is the concentration of the analyte and l is the path length (1.0 cm). The wavelength of maximum absorbance (λ_{max}) for the unbound dye was used for analysis. By rearranging Equation S7, and collecting like terms, the fraction of dye bound can be written as

$$f_b = \frac{\epsilon_{\text{tot}} - \epsilon_f}{\epsilon_b - \epsilon_f} = \frac{A/[L_0] - \epsilon_f}{\epsilon_b - \epsilon_f} \quad (\text{S7})$$

The extinction coefficient of free dye, ϵ_f , is known *a priori*, and the extinction coefficient of bound dye, ϵ_b , can be found via linear regression of ϵ_{tot} vs. $1/[N_0]$, in which the y -intercept represents the limit of infinite DNA concentration. Regressions were performed in the high-concentration region, which is well-represented a linear function of inverse concentration.

Since the equilibrium constant can be written in terms of the fraction bound and the number of binding sites occupied by each ligand, n , as

$$K = \frac{[LN]}{([L_0] - [LN])([N_0] - n[LN])} = \frac{f_b [L_0]}{([L_0] - f_b [L_0])([N_0] - n f_b [L_0])} \quad (\text{S9})$$

it can be directly related to the measured absorbance. Equation S8 can then either be rearranged into a linear form (Scatchard plot) in which the equilibrium constant can be determined via linear regression, or alternately, the quadratic equation can be directly solved to determine the fraction bound after addition a as

$$f_{b,a} = \frac{K[N_0] + Kn[L_0] + 1 - \sqrt{K^2[L_0]^2 n^2 - 2nK^2[L_0][N_0] + 2K[L_0]n + K^2[N_0]^2 + 2K[N_0] + 1}}{2nK[L_0]} \quad (\text{S10})$$

and the equilibrium constant obtained via non-linear regression using Equation S10. Nonlinear regression was performed using in-house Matlab code that uses a Metropolis Monte Carlo search of the parameter space for error estimation; the code is provided later in this document.

Circular dichroism measurements for determining the change in DNA structure on binding were performed using a Jasco J-720 circular dichroism spectrometer, fused quartz cuvettes with a 1 mm path length, and a pure TE buffer blank.

Ethidium Bromide binding curves:

The binding curves for the ethidium bromide data shown in Table 5 in the main text are shown in Figure S7:

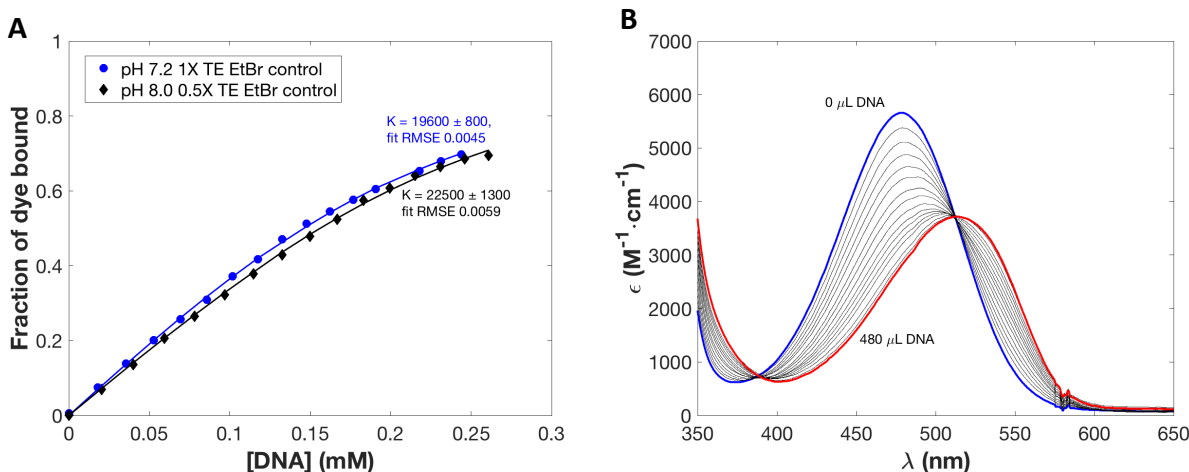


Figure S7. (A) Binding curves for ethidium bromide; (B) spectra from binding titration in pH 8 TAE buffer.

RNA binding:

A preliminary binding titration was run using 30 μL aliquots of ribosomal RNA (1 $\mu\text{g}/\text{mL}$) and an initial solution of 3 mL of 53 μM DANPY-1 in pH 8 TAE buffer and procedures otherwise identical to the DNA binding titrations. While we observed a large shift in the excitation maximum consistent with binding, higher levels of noise in this preliminary experiment prevented calculation of a binding constant. Spectra are shown in Figure S8.

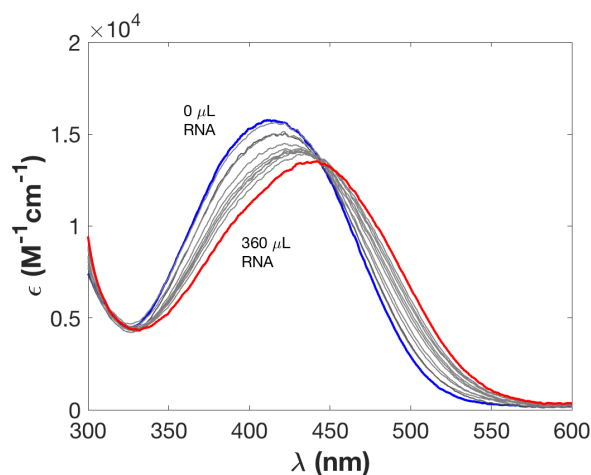


Figure S8. Spectra from RNA binding titration.

Gel electrophoresis and DNA staining:

Materials: The 1kb ladder (1,500 – 100 bp) was obtained from New England Biolabs (Ipswich, MA) while the larger fragment ladders of (10,000 – 500 bp) and (12,000 – 500 bp) were obtained from NE Biolabs and Perfect DNA Markers EMD Millipore (Burlington, MA), respectively.

SeaKem LE agarose was purchased from Lonza (Rockland, ME). The gel casting system (Owl EasyCast B1 Mini Gel Electrophoresis system) was from Thermo Fisher (Waltham, MA). Gels were visualized with a DR46B (viewing surface dimensions: 19 x 15 cm) Dark Reader¹⁹ system from Clare Chemical Research (Dolores, CO) producing blue light in the 400–500 nm range.

Methods: An 0.8% gel was prepared by adding 0.8 gm SeaKem agarose into a 250 ml Erlenmeyer flask that contained 100ml of 0.5X pH 8 TAE buffer (20 mM tris base, 1 mM EDTA, titrated with acetic acid to target pH). The flask contents were brought to a rolling boil by heating in a microwave for 2 minutes. The flask with molten agarose was then placed in a water bath at 45 °C for 10 minutes. The running gel bed was prepared by pouring the semi-cooled contents of the flask into a 7 cm x 8 cm gel tray and the gel was allowed to set for 30 min.

The gel tank was filled with 300 ml of 0.5X TAE, after which the DNA was loaded into wells. Electrophoresis was run at 100 V for 1.5h. If the gel was subjected to in-tank staining, DANPY-1 (96 µg) was placed in the running buffer. Alternatively, if a pre-stained gel was used, 96 µg of DANPY-1 was added directly to the molten agarose, swirled and poured into a gel tray, and no dye was added to the running buffer. The method used most routinely to stain the separated DNA fragments was to post-stain the gel after electrophoresis. Here the gel was placed for at least 30min in 50 ml of 0.5X TAE buffer that contained 92 µg/ml DANPY-1. Unless otherwise specified, all steps of this process were carried out at room temperature. Visualization of the separated DANPY stained DNA fragments was accomplished using a Dark Reader and photographic documentation was made using a BioRad Gel Doc System.

Cell maintenance:

Algae: *Chrysochromulina tobinii* CCMP291:UWCP5.5 (Haptophyta²⁰) *Prorocentrum micans*, *Prorocentrum minimum* (University of Washington Ocean Sciences collection; Pyrrophyta), and *Phaeodactylum tricornerutum* CCMP632 (Heterokontophyta) were used in this study. All algal cultures were maintained in 250 mL Erlenmeyer flasks containing 100 mL of medium that were plugged with silicone sponge stoppers (Bellco Glass, Vineland, NJ) and capped with a sterilizer bag (Proper Manufacturing, Long Island City, NY). All cultures were maintained at 20°C on a 12 hour light:12 hour dark photoperiod under 100 µEm-2s-1 light intensity using full spectrum T12 fluorescent light bulbs (Philips Electronics, Stamford, CT). No CO₂ was provided nor were cultures agitated. Cultures were sampled at approximately hour ~6 in the light portion of the 12 hr light:12 hr dark photoperiod for assessing cell counts and for recovering aliquots for microscopic analysis. Cell counts were accomplished on an Accuri C flow cytometer (BD Scientific, Ann Arbor, MI) using an excitation wavelength of 488nm. *Chrysochromulina tobinii* was grown in a proprietary medium (RAC5) whereas f/2 medium²¹ was used for *Phaeodactylum tricornerutum*, (with Si added) as well as for *Prorocentrum minimum* and *Prorocentrum micans* (without Si addition).

Giardia lamblia trophozoites, strain WB clone 6 (ATCC 50803; American Type Culture Collection) was axenically cultured in TYI-S-33 medium supplemented with bile²² at 37°C. Cultures were maintained in 13mL of medium in 16mL round-bottom screw-cap tubes (Falcon, Denver, CO).

Saccharomyces cerevisiae cells were generously provided by Dr. Jennifer Nemhauser's laboratory at the University of Washington and maintained on YTA (yeast tryptone agar) plates at 37°C.²³

HeLa cells were generously provided by Prof. Marcel Ameloot's laboratory at the University of Hasselt and cultured under standard conditions in DMEM with 10% fetal calf serum. Cells were washed twice with warm PBS and introduced to fresh DMEM medium before imaging. Procedures were identical to those in De Meulenaere et al.,¹⁷ and experiments on DANPY-1 were performed concurrently with the referenced experiments.

Microscopic analyses:

Linear fluorescence: *Prorocentrum micans*, *Prorocentrum minimum*, and *Phaeodactylum tricornutum*, were stained using 15 µM, 1 µM, and 0.5 µM DANPY-1 in H₂O, respectively. Immediately after being stained, cells were placed on a glass microscope slide (Fisher Scientific, Pittsburgh, PA), a high precision cover glass (Zeiss, Lauda-Königshofen, Germany) was gently placed on the cells, and the edges of the cover glass were sealed with silicone vacuum grease (Beckman Coulter, Indianapolis, IN). Cells were immediately examined using 435/48 nm excitation and 597/45 nm emission filter with a DeltaVision Elite microscope (GE, Issaquah, WA) using a 100 x 1.4NA objective, and a sCMOS 5.4 PCIe air-cooled camera (PCO-TECH, Kelheim Bavaria, Germany).

Giardia lamblia, cells were chilled with ice for 25 min to detach them from the culture tube, placed into an AttoFluor cell chamber (Molecular Probes, Eugene, OR), and incubated in a GasPak EZ anaerobic pouch (BD, Sparks, MD) for 1-2 hr at 37 °C. Cells were then washed three times with 1X HBS (Hepes-buffered saline, pH7) before being overlaid with 1X HBS. *G. lamblia* cells were stained using 0.5 µM DANPY-1 in 1X HBS. Imaging was conducted under 2.5% O₂, 5% CO₂, and 37°C (Boldline CO₂/ O₂; Oko Lab, Pozzuoli, Italy). Cells were immediately examined using 435/48 nm excitation and 597/45 nm emission filter with a DeltaVision Elite microscope (GE, Issaquah, WA) using a 100 x 1.4NA objective, and a sCMOS 5.4 PCIe air-cooled camera (PCO-TECH, Kelheim Bavaria, Germany).

Saccharomyces cerevisiae, cells were transferred from YTA plates²³ at 37 °C to 1X HBS and stained with 10µM DANPY-1 in 1X HBS. Immediately after being stained, cells were placed on

a glass microscope slide (Fisher Scientific, Pittsburgh, PA), a high precision cover glass (Zeiss, Lauda-Königshofen, Germany) was gently placed on the cells, and the edges of the cover glass were sealed with silicone vacuum grease (Beckman Coulter, Indianapolis, IN). Cells were immediately imaged at 37 °C under atmospheric conditions (Boldline CO₂/ O₂; Oko Lab, Pozzuoli, Italy) using 435/48nm excitation and 597/45nm emission filter with a DeltaVision Elite microscope (GE, Issaquah, WA) using a 100 x 1.4NA objective, and a sCMOS 5.4 PCIe air-cooled camera (PCO-TECH, Kelheim Bavaria, Germany).

TPEF/SHG: TPEF and SHG microscopy were conducted at Hasselt University and performed using a Zeiss inverted confocal microscope and an 810 nm Mai-Tai laser as the excitation source. HeLa cells were imaged on glass slides and stained using 7 μM DANPY-1 in DMEM with 1% DMSO to aid in membrane penetration. Imaging was conducted in a temperature-controlled environment and under the conditions described in De Meulenaere et. al.¹⁷ Cells were imaged in Petri dishes with ultra-thin bottom, in Phenol Red free medium, usually 30-50 mins after staining. In a subset of the experiments the cells were exposed continuously to mild imaging conditions to study the method of entry and the timing of appearance of TPEF and SHG signal in different cell compartments. In these experiments, the cells were first located based on auto-TPEF, then dye was added about 1 minute after the start of imaging. A rotating half-wave plate was used during imaging to vary polarization of the incident light.

Time-evolution of SHG signal:

The localization of SHG signals was observed to vary over time. Figure S9 shows TPEF and SHG micrographs of a population of HeLa cells shortly after the appearance of the SHG signal (35 min) and near the end of the experiment (55 min).

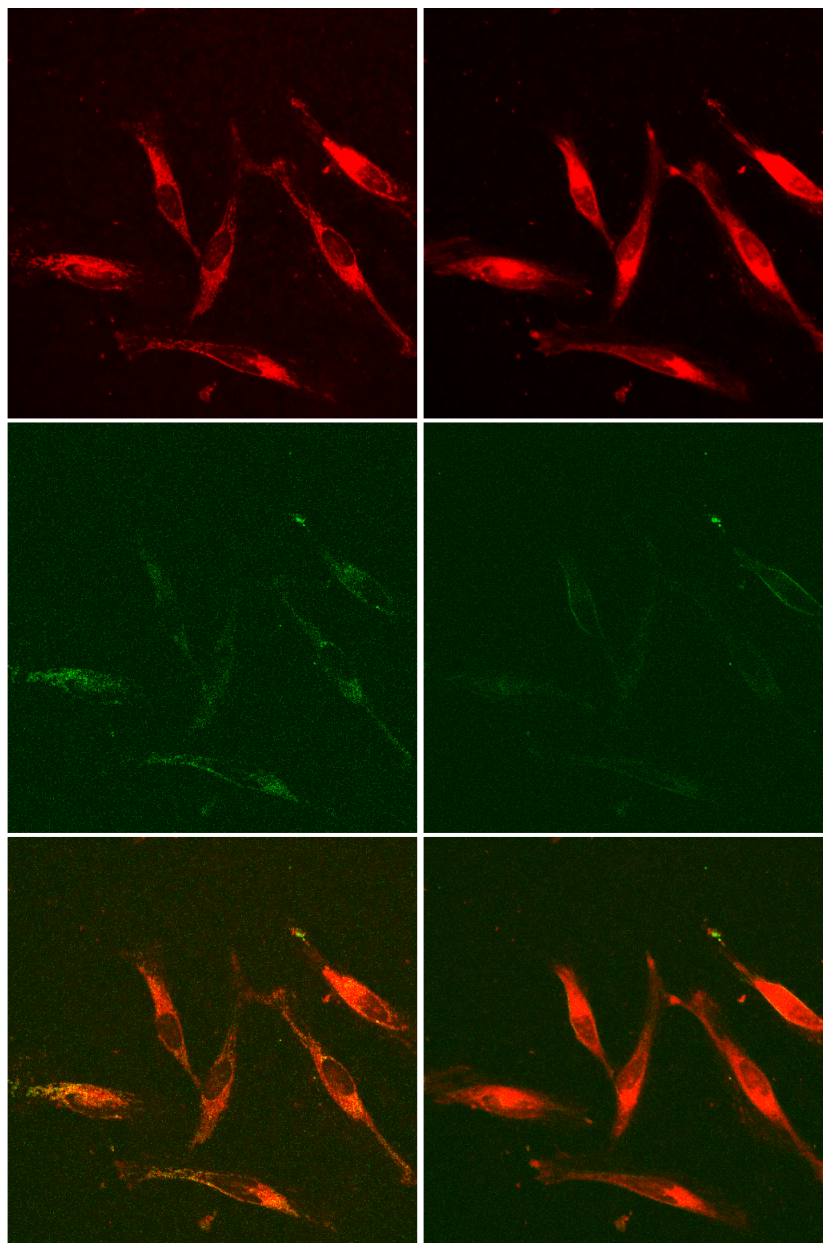


Figure S9. TPEF (top row, red), SHG (middle row, green) and composite (lower row) images of HeLa cells stained with DANPY-1 for 35 minutes (left column) and 55 minutes (right column). The images at 35 min show a SHG signal in regions where endoplasmic reticulum and/or mitochondria are typically observed; by 55 minutes, the signal is no longer prominent in these regions but is primarily observed in the plasma membrane. The images at 55 minutes are averaged over 3 polarizations (25° , 45° , and 65°) to show more of the membrane.

MCFit Nonlinear Fitting Code:

The following Matlab code was used for fitting binding data; it is a general-purpose multi-parameter nonlinear fitting code. The code for the identical and independent binding model function (Equation 8) is also included.

%FITTING CODE

```
function [y, opt_param, errlog, RMSE] = mcfit_2d2(x_data, y_data, pardata, ff, mctype, filtype, maxiter, tol)
%[y, opt_param, errlog, RMSE] = mcfit_2d2(x_data, y_data, pardata, ff, xrow, mctype, filtype, maxiter, tol)
%
%MCfit 2018 multi-parameter nonlinear optimizer
%Version 2d2, 07/2018. Developed by LEJ and NWB
%
% This function uses a fast Monte Carlo minimizer to perform least-squares
%regression on any function of a single variable, with one or more
%optimizable parameters, attempting to find a local best fit based on an
%initial guess for each parameter and constraints on the domain of each
%parameter.
%
%Input variables
% x_data - (m x n array) Independent variable data for m independent
%variables and n points of data.
% y_data - (1 x n array) Dependent variable data
% par_data - (4 x k array) Parameter data, including initial guess, min,
% max, scale factor, for all k parameters. If the min and max in a column
% are the same, the parameter will be treated as a constant.
% ff - fitting function (external m-file, e.g. @fbaux for fbaux.m)
% mctype - (int) Use 1 for simple minimization, 2 for Metropolis (rec.)
% filtype - (int) Use 1 for 3-point moving average (rec.), 2 for FFT
% maxiter - maximum iterations
% tol - relative convergence tolerance compared to noise in function
%
%Output variables
%
% y (1 x n array) - fitted values of dependent variable using optimized
%parameters.
% opt_param (2 x k array) - Values of optimized parameters and fitting
% uncertainty.
% var (1 x iter array) - sum of squares as a function of MCfit iteration,
%used for tracking convergence.
% RMSE (double) - root mean square error of fit (goodness of fit metric)
%
% The y-data must be a single-row array, and the x-data may must be arranged
%in rows, but any number of rows may be used. The parameter data array must
%contain at least one row with the initial guess for the parameter. The
%second and third rows define minimum constraints, and the fourth row
%defines a scale factor for controlling the initial step size for varying
%the parameter (1 means use default grid). The function which the
%optimizer is used to fit must also be declared in the call, and must yield
%y as a function of the x-values and any given parameters. It must be of
%the form y = f(x_data, pardata), and must be called with a function
```

```

%handle e.g. @fit_function. Quotation marks should NOT be used.
% The user must also select a Monte Carlo method; mctype 1 uses simple
%minimization (always accepts lowest variance), whereas mctype 2 uses
%Metropolis-like sampling, with beta being set as 1 over the initial
%interpolated variance. Use of MCtype = 2 is strongly recommended as it
%provides an error estimate and is less likely to get stuck at a local
%minimum, though MCtype1 is retained in the event of convergence issues.
%MCtype 2 is the default.
%
%The tolerance parameter is a simple scaling factor for setting the
%convergence criterion automatically based on the amount of noise in the
%fuction. The default tolerance parameter of 2 (i.e. 2x the difference
%between the initial and smoothed functions) is intended for use with the
%moving average filter; much tighter parameters are often needed when using
%an FFT-based filter; somewhere in the 0.5 to 0.1 range is usually a good
%starting point. However, in most situations the moving average filter
%(filttype = 1) is recommended.
%
%
disp('MCfit 2018 multi-parameter nonlinear fit algorithm')

%Check number of arguments and assume values for missing ones. Also fix
%invalid values.

%Convergence tolerance
if nargin < 8
    tol = 2;
    disp('No convergence tolerance provided, assuming 2x initial noise.')
elseif tol < 0
    disp('Warning - tolerance must be positive. Taking absolute value')
    tol = abs(tol);
elseif tol == 0
    error('Convergence tolerance must be >0')
end

%Maximum iterations
if nargin < 7
    maxiter = 5000;
    disp('No run length limit provided, assuming 5000 iterations')
elseif maxiter < 0
    disp('Warning - maximum number of iterations must be positive. Taking absolute value.')
    maxiter = abs(maxiter);
elseif maxiter < 1
    error('Cannot do anything in zero iterations!')
elseif maxiter < 100
    disp('Warning - small number of maximum iterations. May be less likely to converge.')
end

if maxiter ~= round(maxiter)
    disp('Warning - maximum number of iterations must be an integer. Rounding to nearest integer.')
    maxiter = round(maxiter);
end

%Filter type
if nargin < 6

```

```

    filtype = 1;
    disp('Assuming 3-point moving average')
elseif filtype ~=1 && filtype ~=2 && filtype ~=3
    disp('Warning - invalid MC type; must be 1 (moving avg.), 2 (FFT), or 3 (Savitzky-Golay). Assuming moving avg.')
    filtype = 1;
end

%Monte Carlo type
if nargin < 5
    mctype = 2;
    disp('Assuming Metropolis.')
elseif mctype ~=1 && mctype ~=2
    disp('Warning - invalid MC type; must be 1 (direct) or 2 (Metropolis). Assuming Metropolis.')
    mctype = 2;
end

%Check for input data
if nargin < 4
    error('Cannot run w/o data and/or a fitting function. Please check inputs.')
end

%Build parameter data array and check bounds
if size(pardata,1) == 1
    fprintf('Only initial guess specified; assuming bounds are ± 10x initial guess.\n')
    par_tmp = zeros(4,size(pardata,2));
    par_tmp(1,:) = pardata;
    par_tmp(2,:) = -10*abs(pardata);
    par_tmp(3,:) = 10*abs(pardata);
    par_tmp(4,:) = ones(4,size(pardata,2));
    pardata = par_tmp;
else
    fprintf('Checking initial guesses and bounds...\n')
    if size(pardata,1) < 3 || size(pardata,1) > 4
        error('Invalid size for parameter array; must be exactly 1 (guess), 3 (guess; min ; max), or 4 (guess, ; min ; max ; scale) rows.')
    end
end

%Upper bound must be larger than lower; if the same, fix as constant.
for i = 1:size(pardata,2)
    is_constant = zeros(1,size(pardata,2));
    if pardata(2,i) > pardata(3,i)
        disp(['Warning - the upper bound for parameter ',num2str(i),' is smaller than the lower bound. Transposing.'])
        temp = pardata(2,i);
        pardata(2,i) = pardata(3,i);
        pardata(3,i) = temp;
    elseif pardata(2,i) == pardata(3,i)
        if (pardata(2,i) == pardata(3,i))
            disp(['Fixing parameter ' num2str(i) 'as a constant with value ' num2str(pardata(1,i))])
            is_constant(i) = 1;
        else
            disp(['Warning: The upper and lower bounds for parameter ',num2str(i),' are the same. Will be treated as constant.'])
            is_constant(i) = 1;
        end
    end
end
end

```

```

%Make sure the parameters are all within bounds
if pardata(1,i) > pardata(3,i) || pardata(1,i) < pardata(2,i)
    error(['The value for parameter ',num2str(i),' is out of your specified bounds.'])
end
end

    %Check scaling factors or insert if not present
    if size(pardata,1) == 3
        pardata = [pardata ; ones(1,size(pardata,2))];
    else
        if any(pardata(4,:)) < eps
            error('Scaling factors must be positive real numbers.')
        elseif any(pardata(4,:)) > 1000 || any(pardata(4,:)) < 0.001
            disp('Warning: Very large or small step size scaling factors are likely to delay or prevent convergence.')
        end
    end
end

%Check that input data is oriented correctly
if size(y_data, 1) > 1
    if size(y_data, 2) == 1
        disp('Warning - y_data must be a row vector. Transposing.')
        y_data = y_data';
    else
        error('y_data must consist of a single row.')
    end
end

disp('Smoothing data...')

%Determine final convergence criterion by using smoothed function to estimate
%noise. Two approaches are available; a 3-point moving average or an
%exponentially weighted Fourier transform. The moving average is
%recommended for most data but the FFT is retained for periodic data and
%legacy purposes.

%Set initial values for parameters and scale factors
test_param = pardata(1,:);
scale_factors = pardata(4,:);

%Data filtering
if filtype == 1
    %3-point moving average filtering (requires curve fitting toolbox)
    y_smooth = smooth(y_data,3);
elseif filtype == 2
    %FFT filtering
    sf=1; %Smoothing factor - may be tweaked if poor smoothing
    y_ft=fft(y_data);
    expf=exp(-linspace(0,1,length(y_data))*sf);
    y_filtered = y_ft.*expf;
    y_smooth=real(ifft(y_filtered));
elseif filtype == 3
    %5-2 Savitzky-Golay smoothing (requires curve fitting toolbox)
    y_smooth = smooth(y_data,'sgolay');
end

```

```

%Calculate critical variance
squares=(y_smooth-y_data).^2;
SS_smooth = sum(squares);
converge = abs(SS_smooth*tol);

disp('Beginning optimization...')

%Define index and grid scaling factor (power of 10) for each stage of the
%Monte Carlo loop. Final is simply a flag used for checking convergence.
idx = 1;
grid = 0;
final = 0;
equil = 10000;

%Define flag for random grid search. This kicks on if no
%convergence is seen after a certain number of steps, and randomly guesses
%grid sizes until the function starts converging. Interestingly, this is
%sometimes faster than the systematic method. Feel free to play around with
%this flag. 0 means 'off,' 1 searches between m*1E-5 and m*1E5 of m,
%2 searches between m*1E-25 and m*1E25 of m.

random = 0;
counter = 0;

%Generate fit arrays for the parameter constant and the variance.
parvec=zeros(length(test_param), maxiter);
parvec(:, 1) = test_param';
var=zeros(1, maxiter);
avgvar = zeros(1, maxiter);

%Calculate initial guess for local optimizer. Install a catch line to make
%sure that the array for holding y is generated if the initial guess for
%the parameters is exactly correct. This shouldn't happen outside of
%testing.
y_guess = feval(ff,x_data,test_param);
y = y_guess;

%Calculate variance and sum of squares for initial guess
squares=(y_guess-y_data).^2;
SS = sum(squares);
var(1) = SS;
avgvar(1) = SS;
RMSD_initial = sqrt(SS/length(y_data));
fprintf('The RMSD between the initial and smoothed data is %f\n',RMSD_initial)

%Define initial stage progression criterion
crit = SS/10;

%Check to see if variance is real
if imag(SS) ~=0
    disp('Warning - Imaginary variances detected. Optimizing in complex space.')
end

%Local optimization Monte Carlo loop

%Generate an array to hold parameter data while it is being modified.

```

```

newpar = test_param;
%Allocate memory for average parameter data
avgpar = zeros(equil, length(newpar));
errlog = zeros(maxiter);
avgidx = 1;

%Define sign of initial guessawa
sig = sign(rand(1, length(newpar))-0.5);

while idx < maxiter

    %Iterate the index
    idx = idx + 1;

    for i = 1:length(newpar)

        %Vary parameters one at a time based on the grid spacing, then make
        %sure they are within the user-specified upper and lower bounds.
        %Otherwise, vary them again until an acceptable value is found or
        %100 tries are reached. If the initial guess is not working
        %properly, search over the entire allowed range for the parameters.
        %Only vary parameters if they are not constant.
        ok = 0;
        dparcount = 0;

        if ~(is_constant(i))
            while ok == 0

                if random == 2
                    %Search over all acceptable values if initial guess
                    %disregarded
                    newpar(1,i) = pardata(3,i)-pardata(2,i)*rand;
                else
                    %Otherwise, change one of the parameters based on the grid
                    %spacing and current value of parameter.
                    dpar = sig(1,i)*scale_factors(1,i)*rand*(10^grid).*test_param(1,i);
                    newpar(1,i) = test_param(1,i) + dpar;

                    %Check to see if the guess is within bounds
                    if ((pardata(2,i) <= newpar(1,i)) && (newpar(1,i) <= pardata(3,i)))
                        ok = 1;
                    else
                        dparcount = dparcount+1;
                    end

                    %Crash if unable to find an acceptable guess
                    if dparcount >1000
                        fprintf(['Abnormal termination. Ending parameter values are: ',num2str(test_param),'\n'])
                        fprintf('Current RMSE: %f\n', sqrt(SS/length(y_data)));
                        error('Unable to iterate function without exceeding bounds. Try a different initial guess or change
bounds.')

```

```

%Calculate new guess
y_new = feval(ff,x_data,newpar);

%Calculate new variance and sum of squares
squares = (y_new-y_data).^2;
SS_new = sum(squares);

%Compare variances and determine sign of change. Accept change if the
%variance is smaller, and if the guess is accepted, maintain the sign
%of the change for the next guess. %If Metropolis sampling is used,
%apply Metropolis criterion for acceptance of higher-variance guesses.

%Direct minimization criterion
if abs(SS_new) < abs(SS)
    sig(i) = sign(newpar(i) - test_param(i));
    test_param = newpar;
    y=y_new;
    SS = SS_new;

%Metropolis criterion
elseif mctype == 2 && rand < exp(-(abs(SS_new) - abs(SS))/SS_smooth)
    test_param = newpar;
    sig(i) = sign(newpar(i) - test_param(i));
    y=y_new;
    SS = SS_new;
else
    %Randomize the sign of the next kick for the parameter if the
    %guess was not accepted.
    sig(i) = sign(rand-0.5);
end
end

%Record the value of the parameter and sum of squares for the step
parvec(:,idx) = test_param';
errlog(idx) = abs(SS);

%Check if the average or final variance dropped. If so, reset the
%counter used for turning on the random grid search to 0. Otherwise,
%advance it by 1.
if avgvar(1, idx) < avgvar(1, idx-1)
    counter = 0;
elseif var(1, idx) < var(1, idx -1)
    counter = 0;
else
    counter = counter + 1;
end

%Shrink grid size as function converges
if (random == 0 && final == 0 && (abs(SS) < crit) && counter > 10)
    fprintf('Stage complete after %i iterations.\n',idx)
    fprintf('Current RMSE: %f\n', sqrt(SS/length(y_data)));
    grid = grid - 1;
    crit = crit/100;
elseif random == 1 && abs(SS) < crit
    disp('Random grid off.')
    random = 0;

```



```

end
%Test for convergence and activate final optimization if convergence
%criterion reached.
if abs(SS) <= converge && final == 0
    fprintf('\nPreliminary convergence reached after %i iterations.\n',idx)
    fprintf(['Parameter values are: ',num2str(test_param),'\n'])
    fprintf('Current RMSE: %f\n', sqrt(SS/length(y_data)));
    %Change maximum iterations so the algorithm will stop after the
    %designated equilibration time. If the algorithm is about to run
    %out of iterations, use the remaining iterations as the
    %equilibration time.
    if idx < maxiter - equil
        maxiter = idx+equil;
    else
        equil = maxiter - idx;
    end
    fprintf('Fine-tuning for next %i iterations.\n\n',equil)

    final = 1;
    grid = grid - 1;
    SS_smooth = SS_smooth/log(10);
end

%If converged, record the parameters for calculating the average
%values.
if final == 1 && mctype == 2
    avgpar(avgidx, :) = test_param;
    avgidx = avgidx + 1;
end

%If grid randomizer is active, set new grid size
if random == 1
    grid = ceil(10*rand)-5;
    crit = SS/10;

%If convergence is slow, randomize the grid size to attempt to get
%unstuck.
elseif grid == 0 && counter > 50 && random == 0
    random = 1;
    disp('Warning - poor initial guess. Attempting to converge using random grid.')
end

%If completely stuck, ignore the initial guess and randomize
if random == 1 && counter > 200
    random = 2;
    disp('Warning - no progress in last 200 iterations. Disregarding initial guess.')
end

end

%Prune the variance and parameter arrays to only contain elements for the
%number of iterations actually run
errlog = errlog(2:idx);
avgpar = avgpar(1:(avgidx-1),:);

%Calculate the average values of the parameters after convergence. If

```

```

%Metropolis sampling is used, return the average value after
%equilibration, if simple minimization is used, return the final value.
%Also calculate the standard deviation of each parameter during
%equilibration. Note that this is not a formal regression statistic.
if mctype == 2 && final == 1
    opt_param(1,:) = mean(avgpar, 1);
    opt_param(2,:) = std(avgpar, 0, 1);
else
    opt_param(1,:) = test_param;
    opt_param(2,:) = 1/0;
end

%Calculate MSE and RMSE from SS
MSE = SS/length(y_data);
RMSE = sqrt(MSE);

%Output data

%Display warning if convergence criteria not met
if final ~= 1
    fprintf('Warning - Convergence criteria not met. The final sum of squares after %i iterations is: %f\n', idx, abs(SS))
    fprintf('The critical sum of squares was: %f\n',converge)
else
    fprintf('Final convergence reached versus a critical sum of squares of %f\n',converge)
end

%Display output. If Metropolis criterion is used, also display the standard
%deviation of the parameters during equilibration. Also show the final sum
%of squares (simple) or average sum of squares (Metropolis)
fprintf('The final grid size was 10^%f\n',grid)

if final==1
    fprintf('The final optimized values of the parameters after %i iterations are:\n', idx)
    disp(opt_param(1,:))
    if mctype == 2
        fprintf('The standard deviation of each parameter during equilibration is:\n')
        disp(opt_param(2,:))
        SS = mean(errlog(idx-equil:(idx-1)));
        fprintf('The final average sum of squares based on equilibration with the amount of noise in the data is: %f\n',SS)
    else
        fprintf('The final sum of squares is: %f\n',SS)
    end
    fprintf('The MSE of the fit is: %f\n', MSE)
    fprintf('The RMSE of the fit is: %f\n', RMSE)
else
    disp('The last recorded values of the parameters are:')
    disp(test_param)
end

disp('Done.')

%BINDING MODEL
function y = isbm(NOL0, pars)
%y = isbm(NOL0, pars)

%Identical binding site model for biological equilibria

```

```
%Total concentration of macromolecule (N0) and ligand (L0)
N0 = N0L0(1,:);
L0 = N0L0(2,:);

%Equilibrium constant
K = pars(1);

%Number of sites excluded by a ligand. n_ex=1 for 1:1 binding, n_ex=2 for
%nearest neighbor excluded model
n_ex = pars(2);

%Binding equation
y = ((K*n_ex*L0+K*N0+1)-((((-K*n_ex*L0-K*N0-1).^2)-4*(K^2)*n_ex*L0.*N0).^(1/2)))/(2*n_ex*K*L0);
```

Coordinates for electronic structure calculations (xyz format):DANPY-1 cation M062X/6-31+G(d) in PCM dichloromethane (+1 singlet)

C	1.21670	0.33820	-0.06490
H	0.75410	-1.75000	0.18460
C	0.36020	-0.74510	0.04970
C	-0.70030	1.82850	-0.22100
C	-1.03910	-0.57770	0.04320
C	0.65560	1.64420	-0.19630
C	-1.59870	0.72650	-0.09910
C	-1.93320	-1.67580	0.17830
H	1.31020	2.50270	-0.31510
H	-3.38220	1.90840	-0.21930
H	-1.11110	2.82760	-0.34180
C	-3.28820	-1.49760	0.16340
H	-1.52330	-2.67640	0.29270
H	-3.93270	-2.36260	0.26580
C	-3.86520	-0.18880	0.01050
C	-2.99660	0.90070	-0.11340
C	2.67080	0.14730	-0.03500
N	5.43460	-0.21980	0.03450
C	3.26930	-1.05060	-0.47310
C	3.53810	1.15100	0.43180
C	4.89970	0.94350	0.45720
C	4.63410	-1.20650	-0.42570
H	2.67590	-1.86010	-0.88150
H	3.15970	2.09390	0.80810
H	5.59480	1.68930	0.82310
H	5.13330	-2.10910	-0.75930
N	-5.22230	-0.03650	-0.01250
C	6.89080	-0.44670	0.09120
H	7.22870	-0.81310	-0.87780
H	7.10420	-1.18110	0.86860
H	7.38570	0.49460	0.32140
C	-5.78620	1.29480	-0.13380
H	-5.44240	1.78250	-1.05360
H	-5.51060	1.92980	0.71910
H	-6.87210	1.22020	-0.17400
C	-6.09960	-1.17080	0.22500
H	-7.13260	-0.82650	0.19700
H	-5.91750	-1.62620	1.20650
H	-5.97790	-1.94010	-0.54600

DANPY-1 cation M062X/6-31+G(d) in PCM methanol (+1 singlet)

C	1.21680	0.33940	-0.06480
H	0.75670	-1.74790	0.18970

C	0.36170	-0.74370	0.05290
C	-0.70060	1.82880	-0.22590
C	-1.03860	-0.57670	0.04470
C	0.65590	1.64470	-0.20020
C	-1.59840	0.72660	-0.10170
C	-1.93230	-1.67480	0.18230
H	1.31110	2.50270	-0.32000
H	-3.38320	1.90750	-0.22640
H	-1.11150	2.82750	-0.34940
C	-3.28780	-1.49720	0.16510
H	-1.52200	-2.67470	0.30080
H	-3.93180	-2.36230	0.27040
C	-3.86540	-0.18950	0.00680
C	-2.99740	0.90000	-0.11770
C	2.67270	0.14850	-0.03480
N	5.43370	-0.22060	0.03610
C	3.26940	-1.04560	-0.48270
C	3.53790	1.14790	0.44210
C	4.89990	0.93920	0.46810
C	4.63450	-1.20280	-0.43430
H	2.67580	-1.85130	-0.89810
H	3.15910	2.08800	0.82470
H	5.59500	1.68110	0.84140
H	5.13370	-2.10290	-0.77420
N	-5.22360	-0.03870	-0.02130
C	6.89010	-0.44820	0.09000
H	7.23080	-0.78360	-0.88910
H	7.10020	-1.20690	0.84450
H	7.38270	0.48570	0.35230
C	-5.78760	1.29350	-0.13110
H	-5.44380	1.78890	-1.04670
H	-5.51210	1.92230	0.72660
H	-6.87350	1.21900	-0.17220
C	-6.09940	-1.17110	0.23090
H	-7.13300	-0.82940	0.19230
H	-5.92070	-1.61210	1.21990
H	-5.97260	-1.95140	-0.52780

DAST cation M062X/6-31+G(d) in PCM acetonitrile (+1 singlet)

H	-1.11250	1.90050	0.02560
C	-1.71060	0.99390	0.01180
C	-3.30160	-1.29380	-0.02010
C	-1.08390	-0.26860	-0.00760
C	-3.08460	1.12320	0.01580
C	-3.92870	-0.02170	0.00010
C	-1.92260	-1.39880	-0.02290

H	-3.51370	2.11780	0.03260
H	-1.47420	-2.39000	-0.03800
H	-3.89590	-2.19930	-0.03220
C	0.35230	-0.45430	-0.00900
H	0.66920	-1.49690	-0.01200
C	1.30010	0.51550	-0.00870
H	1.00830	1.56270	-0.01400
C	2.72720	0.27460	-0.00440
N	5.50190	-0.05960	0.00760
C	3.61200	1.37210	-0.03160
C	3.32140	-1.00790	0.02890
C	4.68680	-1.14050	0.03390
C	4.97410	1.18150	-0.02620
H	3.23070	2.38680	-0.05760
H	2.72700	-1.91270	0.05420
H	5.17910	-2.10600	0.06060
H	5.67810	2.00460	-0.04920
C	6.96070	-0.26250	0.00600
H	7.23730	-0.85920	0.87530
H	7.44880	0.70870	0.05590
H	7.24810	-0.77650	-0.91180
N	-5.28440	0.10150	0.00500
C	-5.89870	1.41830	0.02700
H	-5.61050	1.97860	0.92460
H	-6.98160	1.30290	0.02950
H	-5.61730	2.00540	-0.85550
C	-6.12040	-1.08670	-0.01340
H	-5.93700	-1.71580	0.86610
H	-5.93980	-1.68600	-0.91410
H	-7.16660	-0.78480	-0.00670

Disperse Red 1 M062X/6-31+G(d) in PCM chloroform (neutral singlet)

H	-2.77850	2.38910	-0.18270
C	-3.31330	1.44730	-0.11270
C	-4.62680	-1.01690	0.05750
C	-2.58090	0.25580	-0.08260
C	-4.70050	1.42160	-0.04950
C	-5.33180	0.18570	0.03500
C	-3.24280	-0.97910	-0.00190
H	-5.28540	2.33330	-0.06560
H	-2.66460	-1.89550	0.01000
H	-5.16160	-1.95740	0.11830
N	-1.16900	0.40000	-0.15690
N	-0.54080	-0.66770	0.02430
C	0.85510	-0.58330	-0.05660
C	3.68410	-0.64150	-0.18000

C	1.58050	0.58730	-0.34350
C	1.55890	-1.77080	0.17400
C	2.94110	-1.80990	0.12040
C	2.95790	0.56300	-0.40100
H	1.04740	1.51680	-0.51470
H	0.99610	-2.67260	0.39950
H	3.44560	-2.75050	0.30250
H	3.48110	1.48890	-0.60840
N	-6.79560	0.14470	0.09970
O	-7.40170	1.20380	0.06090
O	-7.33490	-0.94680	0.19070
N	5.04940	-0.68340	-0.25730
C	5.75680	-1.90040	0.10620
H	6.82940	-1.71260	0.05170
H	5.51660	-2.72120	-0.58010
H	5.51460	-2.21540	1.12840
C	5.83680	0.50180	-0.55350
H	5.33680	1.11230	-1.31090
H	6.78470	0.17610	-0.99500
C	6.10920	1.34130	0.69710
H	6.64390	0.73640	1.44240
H	5.16370	1.66110	1.14480
O	6.82240	2.52460	0.38550
H	7.73060	2.29310	0.14180

Isoc M062X/6-31+G(d) in PCM chloroform (neutral singlet)

H	2.47520	1.76570	0.82840
C	2.09400	0.83400	0.42240
C	1.11120	-1.56030	-0.57440
C	0.72860	0.62230	0.35250
C	2.99890	-0.14920	-0.02350
C	2.48250	-1.35600	-0.52190
C	0.19930	-0.57990	-0.15210
H	0.06590	1.40240	0.71550
H	3.15960	-2.12770	-0.87420
H	0.73360	-2.50000	-0.97120
C	-1.23080	-0.84910	-0.25850
H	-1.47770	-1.84970	-0.61100
C	-2.23550	0.01480	0.01200
H	-2.00580	1.02800	0.33670
C	-3.64680	-0.28470	-0.13840
N	4.38020	0.07850	0.03500
C	-5.96640	0.51790	-0.09440
C	-4.55540	0.70760	0.09040
H	-4.20460	1.68280	0.42010
C	-6.86490	1.51440	0.20490

C	-4.09520	-1.66000	-0.56610
H	-3.45240	-2.42070	-0.10800
H	-3.94900	-1.74460	-1.65420
C	-6.43170	-0.79030	-0.67230
H	-6.37580	-0.70090	-1.76830
H	-7.48210	-0.97550	-0.42250
C	-5.55980	-1.97090	-0.21840
C	-6.00070	-3.23350	-0.96080
H	-5.37570	-4.08660	-0.67270
H	-5.92250	-3.10450	-2.04640
H	-7.04070	-3.48100	-0.72020
C	-5.71860	-2.19280	1.29130
H	-5.39260	-1.32380	1.87260
H	-5.12610	-3.05650	1.61270
H	-6.76750	-2.39150	1.53860
C	5.29430	-1.00300	0.16430
C	7.12170	-3.10670	0.43130
C	5.08450	-1.99920	1.12420
C	6.42380	-1.06300	-0.65840
C	7.33470	-2.10700	-0.51790
C	5.99160	-3.04860	1.24800
H	4.21110	-1.94590	1.76850
H	6.58490	-0.28680	-1.40140
H	8.20990	-2.14170	-1.16020
H	5.82070	-3.81630	1.99710
C	4.90590	1.39270	-0.10610
C	5.98230	3.96040	-0.39310
C	4.42950	2.24710	-1.10600
C	5.92550	1.82740	0.74670
C	6.46380	3.10290	0.59650
C	4.96140	3.52730	-1.23970
H	3.64500	1.90360	-1.77490
H	6.29450	1.15880	1.51970
H	7.25670	3.43010	1.26290
H	4.58450	4.18340	-2.01890
H	7.83160	-3.92130	0.53670
H	6.40070	4.95590	-0.50550
C	-8.27270	1.34900	0.00780
C	-6.44010	2.78360	0.71510
N	-6.08020	3.80530	1.12790
N	-9.41300	1.21380	-0.15330

DANPY-1 cation B3LYP/cc-pVTZ in PCM methanol (+1 singlet)

C	1.21670	0.33820	-0.06490
H	0.75410	-1.75000	0.18460
C	0.36020	-0.74510	0.04970

C	-0.70030	1.82850	-0.22100
C	-1.03910	-0.57770	0.04320
C	0.65560	1.64420	-0.19630
C	-1.59870	0.72650	-0.09910
C	-1.93320	-1.67580	0.17830
H	1.31020	2.50270	-0.31510
H	-3.38220	1.90840	-0.21930
H	-1.11110	2.82760	-0.34180
C	-3.28820	-1.49760	0.16340
H	-1.52330	-2.67640	0.29270
H	-3.93270	-2.36260	0.26580
C	-3.86520	-0.18880	0.01050
C	-2.99660	0.90070	-0.11340
C	2.67080	0.14730	-0.03500
N	5.43460	-0.21980	0.03450
C	3.26930	-1.05060	-0.47310
C	3.53810	1.15100	0.43180
C	4.89970	0.94350	0.45720
C	4.63410	-1.20650	-0.42570
H	2.67590	-1.86010	-0.88150
H	3.15970	2.09390	0.80810
H	5.59480	1.68930	0.82310
H	5.13330	-2.10910	-0.75930
N	-5.22230	-0.03650	-0.01250
C	6.89080	-0.44670	0.09120
H	7.22870	-0.81310	-0.87780
H	7.10420	-1.18110	0.86860
H	7.38570	0.49460	0.32140
C	-5.78620	1.29480	-0.13380
H	-5.44240	1.78250	-1.05360
H	-5.51060	1.92980	0.71910
H	-6.87210	1.22020	-0.17400
C	-6.09960	-1.17080	0.22500
H	-7.13260	-0.82650	0.19700
H	-5.91750	-1.62620	1.20650
H	-5.97790	-1.94010	-0.54600

References for Supporting Information:

1. Johnson, L. E.; Casford, M. T.; Elder, D. L.; Davies, P. B.; Johal, M. S., SFG characterization of a cationic ONLO dye in biological thin films. *Proc. SPIE - Nanobiosystems: Processing, Characterization, and Applications VI* **2013**, 8817, 88170P-88170P-9.
2. Johnson, L. E. Multi-Scale Modeling of Organic Electro-Optic Materials. Doctor of Philosophy, University of Washington, Seattle, 2012.
3. Johnson, L. E.; Latimer, L. N.; Benight, S. J.; Watanabe, Z. H.; Elder, D. L.; Robinson, B. H.; Bartsch, C. M.; Heckman, E. M.; Depotter, G.; Clays, K., Novel cationic dye and crosslinkable surfactant for DNA biophotonics. *Proc. SPIE - Nanobiosystems: Processing, Characterization, and Applications V* **2012**, 8464, 0D1-0D10.
4. APEX2 (Version 2.1-4), SAINT (version 7.34A), SADABS(version 2007/4), BrukerAXS Inc.: Madison, Wisconsin, USA, 2007.
5. Altomare, A.; Burla, C.; Camalli, M.; Cascarno, G. L.; Giacovazzo, C.; Guagliardi, A.; Moliterni, A. G. G.; Polidori, G.; Spagna, R., SIR97: a new tool for crystal structure determination and refinement. *Journal of Applied Crystallography* **1999**, 32, 115-119.
6. Sheldrick, G., Crystal structure refinement with SHELXL. *Acta Crystallographia* **2015**, C71, 3-8.
7. Mackay, S.; Edwards, C.; Henderson, C.; Gilmore, C.; Stewart, N.; Shankland, K.; Donald, A. *Maxias: A computer program for the solution and refinement of crystal structures from diffraction data*, University of Glasgow: Scotland, 1997.
8. Wassmaier, D.; Kirfel, A., New Analytical Scattering Factor Functions for Free Atoms and Ions. *Acta Crystallographia A* **1995**, 51, 416-430.
9. Farrugia, L., ORTEP-3 for Windows. *Journal of Applied Crystallography* **1997**, 30, 565.
10. Frisch, M. J.; Trucks, G. W.; Schlegel, H. B.; Scuseria, G. E.; Robb, M. A.; Cheeseman, J. R.; Scalmani, V. B.; Mennucci, B.; Petersson, G. A.; Nakatsuji, H.; Caricato, M.; Li, X.; Hratchian, H. P.; Izmaylov, A. F.; Bloino, J.; Zheng, G.; Sonnenberg, J. L.; Hada, M.; Ehara, M.; Toyota, K.; Fukuda, R.; Hasegawa, J.; Ishida, M.; Nakajima, T.; Honda, Y.; Kitao, O.; Nakai, H.; Vreven, T.; J. A. Montgomery, J.; Peralta, J. E.; Ogliaro, F.; Bearpark, M.; Heyd, J. J.; Brothers, E.; Kudin, K. N.; Staroverov, V. N.; Kobayashi, R.; Normand, J.; Raghavachari, K.; Rendell, A.; Burant, J. C.; Iyengar, S. S.; Tomasi, J.; Cossi, M.; Rega, N.; Millam, J. M.; Klene, M.; Knox, J. E.; Cross, J. B.; Bakken, V.; Adamo, C.; Jaramillo, J.; Gomperts, R.; Stratmann, R. E.; Yazyev, O.; Austin, A. J.; Cammi, R.; Pomelli, C.; Ochterski, J. W.; Martin, R. L.; Morokuma, K.; Zakrzewski, V. G.; Voth, G. A.; Salvador, P.; Dannenberg, J. J.; Dapprich, S.; Daniels, A. D.; Farkas, Ö.; Foresman, J. B.; Ortiz, J. V.; Cioslowski, J.; Fox, D. J. *Gaussian 09*, Revision A.1; Gaussian, Inc.: Wallingford, CT, 2009.
11. Johnson, L. E.; Dalton, L. R.; Robinson, B. H., Optimizing Calculations of Electronic Excitations and Relative Hyperpolarizabilities of Electrooptic Chromophores. *Accounts of Chemical Research* **2014**, 47 (11), 3258-3265.
12. Fairchild, S. Z.; Bradshaw, C. F.; Su, W.; Guharay, S. K., Predicting Raman Spectra Using Density Functional Theory. *Applied Spectroscopy* **2009**, 63, 733-741.
13. Yang, Y.; Li, D.; Li, C.; Liu, Y.; Jiang, K., Hydrogen bond strengthening induces fluorescence quenching of PRODAN derivative by turning on twisted intramolecular charge transfer. *Spectrochimica Acta Part A: Molecular and Biomolecular Spectroscopy* **2017**, 187, 68-74.
14. Preus, S. *DecayFit - Fluorescence Decay Analysis Software*, 1.4; FluorTools: 2014.

15. Xu, C.; Webb, W. W., Measurement of two-photon excitation cross sections of molecular fluorophores with data from 690 to 1050 nm. *Journal of the Optical Society of America B* **1996**, *13* (3).
16. Albota, M. A.; Xu, C.; Webb, W. W., Two-photon fluorescence excitation cross sections of biomolecular probes from 690 to 960 nm. *Applied Optics* **1998**, *37* (31).
17. De Meulenaere, E.; Chen, W.-Q.; Van Cleuvenbergen, S.; Zheng, M.-L.; Psilodimitrakopoulos, S.; Paesen, R.; Taymans, J.-M.; Ameloot, M.; Vanderleyden, J.; Loza-Alvarez, P.; Duan, X.-M.; Clays, K., Molecular engineering of chromophores for combined second-harmonic and two-photon fluorescence in cellular imaging. *Chemical Science* **2012**, *3* (4), 984.
18. Lunn, G.; Sansone, E. B., Ethidium bromide: Destruction and decontamination of solutions. *Analytical Biochemistry* **1987**, *162* (2), 453-458.
19. Seville, M., A whole new way of looking at things: The use of Dark Reader technology to detect fluorophors. *Electrophoresis* **2001**, *22*, 814-828.
20. Richardson, P. M.; Hovde, B. T.; Deodato, C. R.; Hunsperger, H. M.; Ryken, S. A.; Yost, W.; Jha, R. K.; Patterson, J.; Monnat, R. J.; Barlow, S. B.; Starkenburg, S. R.; Cattolico, R. A., Genome Sequence and Transcriptome Analyses of *Chrysochromulina tobin*: Metabolic Tools for Enhanced Algal Fitness in the Prominent Order Prymnesiales (Haptophyceae). *PLOS Genetics* **2015**, *11* (9).
21. Guillard, R. R. L., Culture of phytoplankton for feeding marine invertebrates. In *Culture of Marine Invertebrate Animals*, Smith, W. L.; Chanley, M. H., Eds. Plenum Press: New York, 1975; pp 26-60.
22. Keister, D. B., Axenic culture of *Giardia lamblia* in TYI-S-33 medium supplemented with bile. *Transactions of the Royal Society of Tropical Medicine and Hygiene* **1983**, *77* (4), 487-488.
23. Sanders, E. R., Aseptic Laboratory Techniques: Plating Methods. *Journal of Visualized Experiments* **2012**, (63).